

Vertex & Tracking Detectors

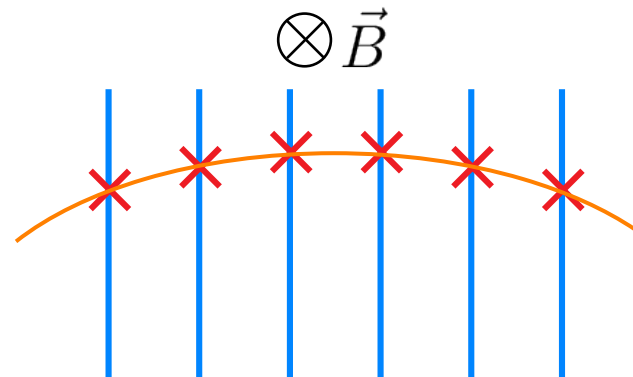
for... vertexing & tracking?

Momentum Reconstruction

- Relativistic particles in magnetic field:
 - $\vec{p} \perp \vec{B}$ circular track
 - $\vec{p} \parallel \vec{B}$ straight track
 - Else helical track
- Lorentz force and centripetal force in equilibrium:

$$\begin{aligned}
 |\vec{F}_L| &= |\vec{F}_Z| \\
 |q\vec{v} \times \vec{B}| &= \frac{m\vec{v}^2}{R} \\
 p_T &= qBR
 \end{aligned}
 \longrightarrow$$

- Measurement of the radius of curved tracks yields *transverse momentum* p_T



Simple approximation

$$p_T = 0.3|z|BR$$

$$[p_T] = \text{GeV}/c$$

with $[R] = \text{m}$

$$[B] = \text{T}$$

$$z = q/e$$

Momentum Measurement

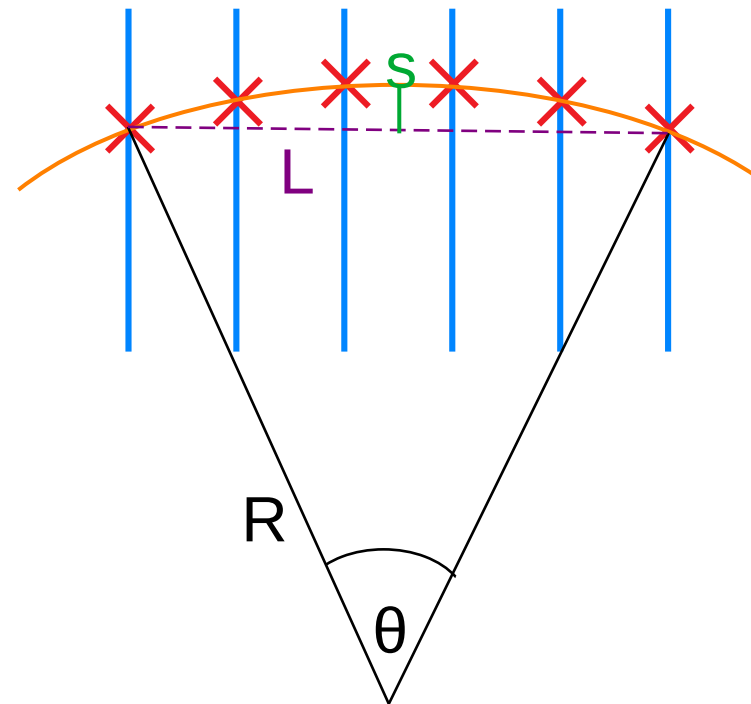
- Radius can be determined by measurement of *sagitta* length s at track length L

$$s \approx \frac{L^2}{8R}$$

- Uncertainty of momentum proportional to uncertainty of sagitta measurement:

$$p = qBR = \frac{8qB}{L^2}s \quad \Rightarrow \quad \sigma_p \propto \sigma_s$$

- Uncertainties of sagitta measurement:
 - Spatial detector resolution
 - Multiple Coulomb scattering**



Multiple Coulomb Scattering

Charged particles traversing medium are **deflected by many small-angle scatterers**

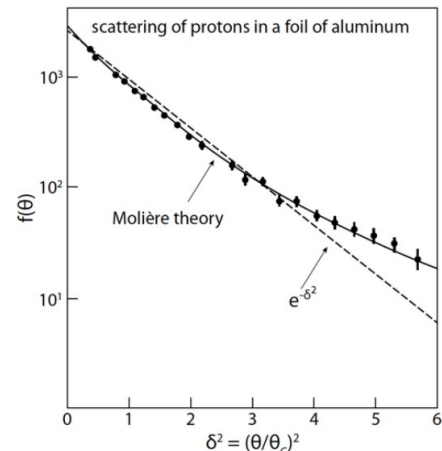
- Deflection off Coulomb potential of nuclei, Rutherford cross section:

$$\left. \frac{d\sigma}{d\Omega} \right|_{\text{Rutherford}} = z^2 Z^2 \alpha^2 \hbar^2 \frac{1}{\beta^2 p^2} \frac{1}{4 \sin^4 \frac{\theta}{2}}$$

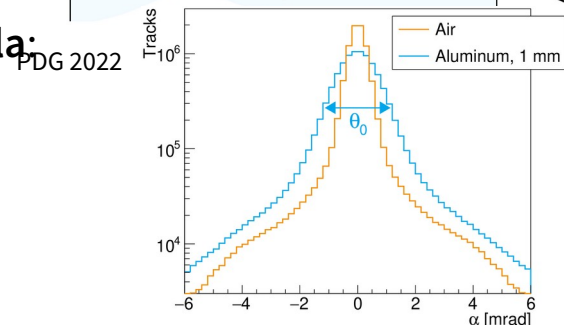
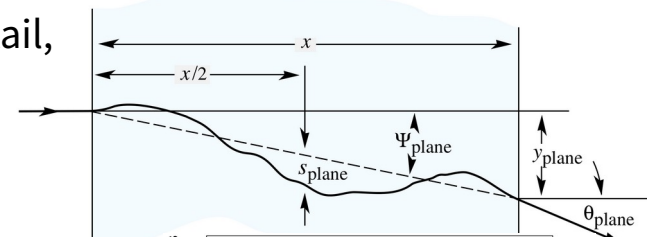
- Many small-angle scatterings → Gaussian distribution of scattering angle (**central limit theorem**)
- Sometimes “hard” scattering with large angle, produce non-Gaussian tail, described by Molière theory

Often a Gaussian approximation is enough,
Standard deviation of distribution can be approximated via **Highland Formula**:

$$\theta_0 = \frac{13.6 \text{ MeV}}{\beta c p} z \sqrt{\frac{x}{X_0}} \left[1 + 0.038 \ln \left(\frac{x}{X_0} \right) \right]$$



H. Bichsel, Phys. Rev. 112, 182

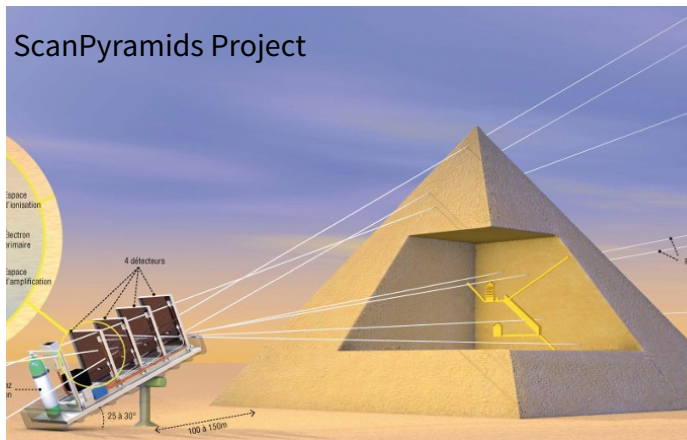


PDG 2022

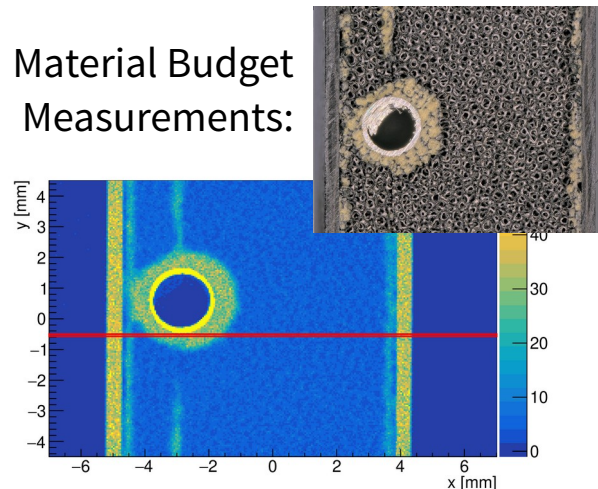
Implications of Multiple Scattering

- Stochastic deflection leads to deterioration of the position resolution for tracking detectors
 - Consequently tracking precision (e.g. momentum resolution is affected)
 - Remedy by using light & thin materials
- Can be used to gain information on traversed objects:

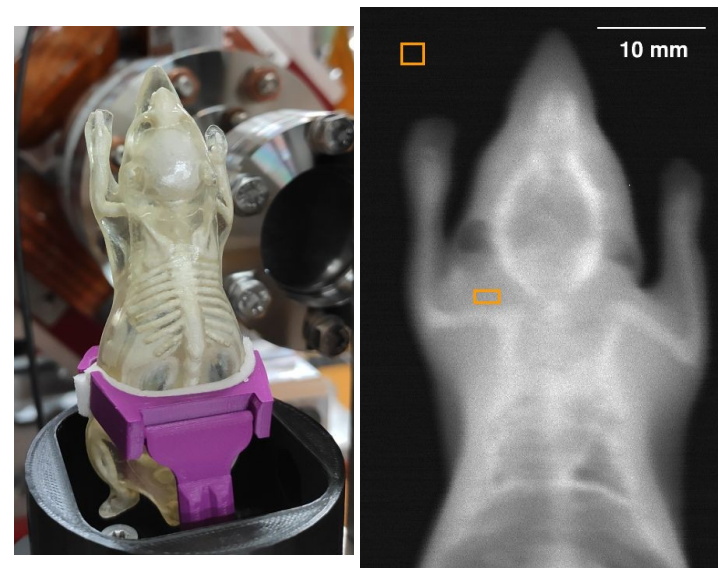
Cosmic Muon Tomography:

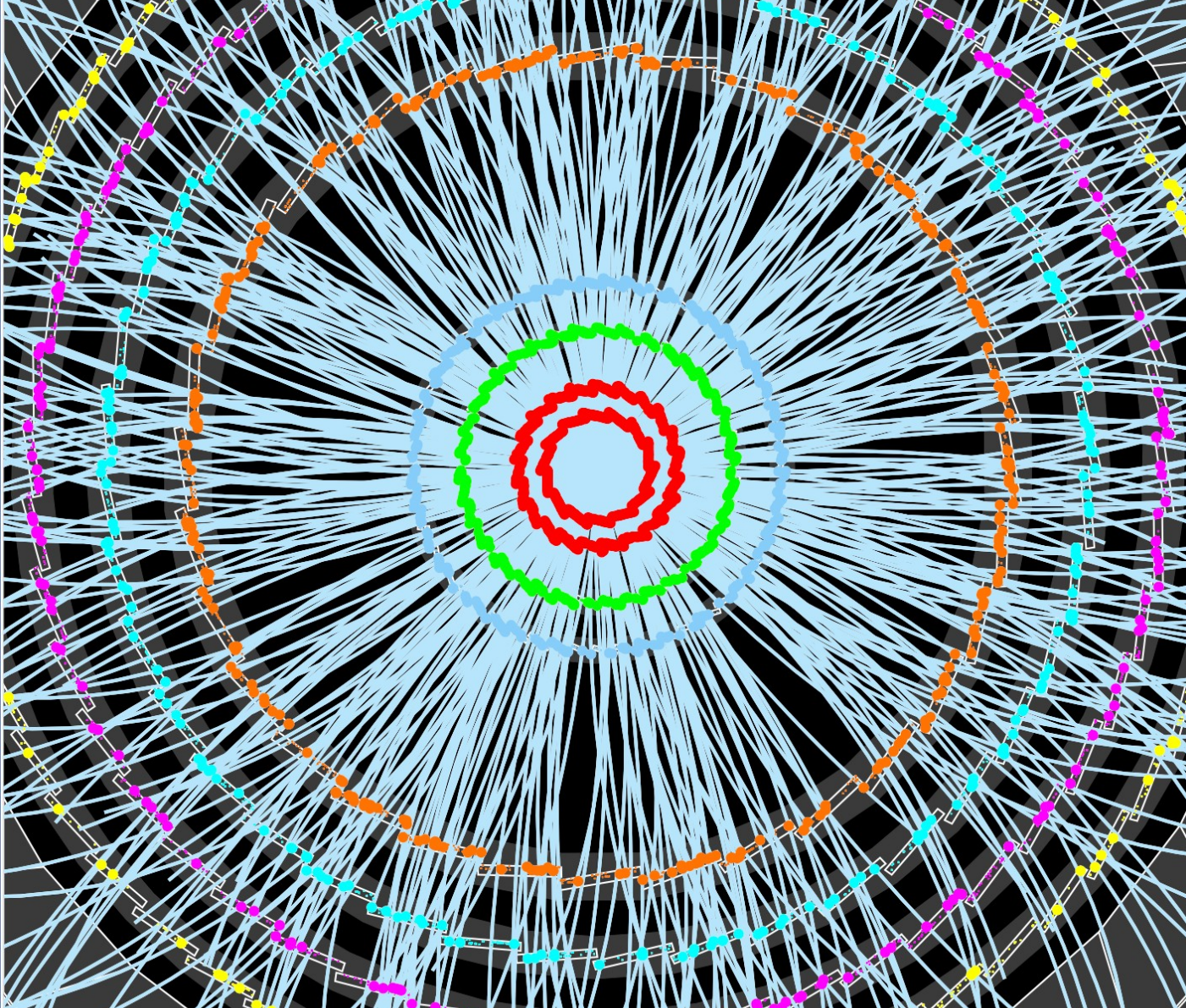


Material Budget Measurements:



Medical Imaging electron CT:



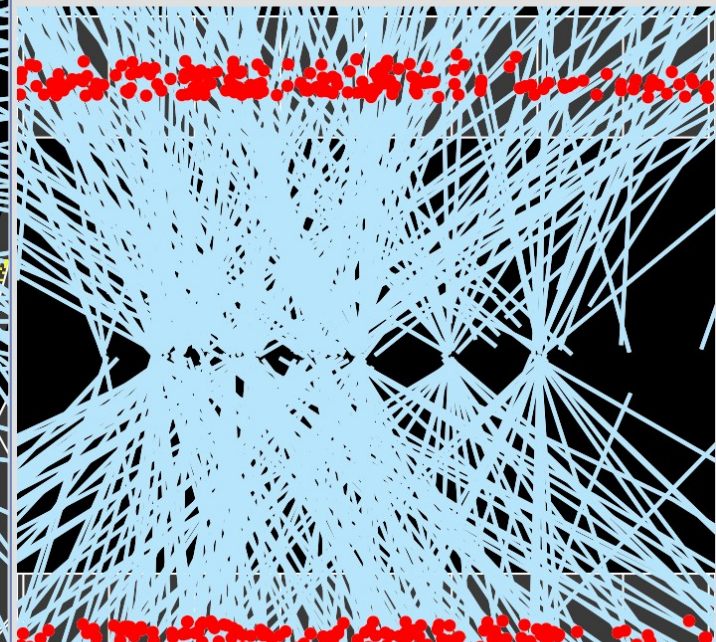


ATLAS

EXPERIMENT

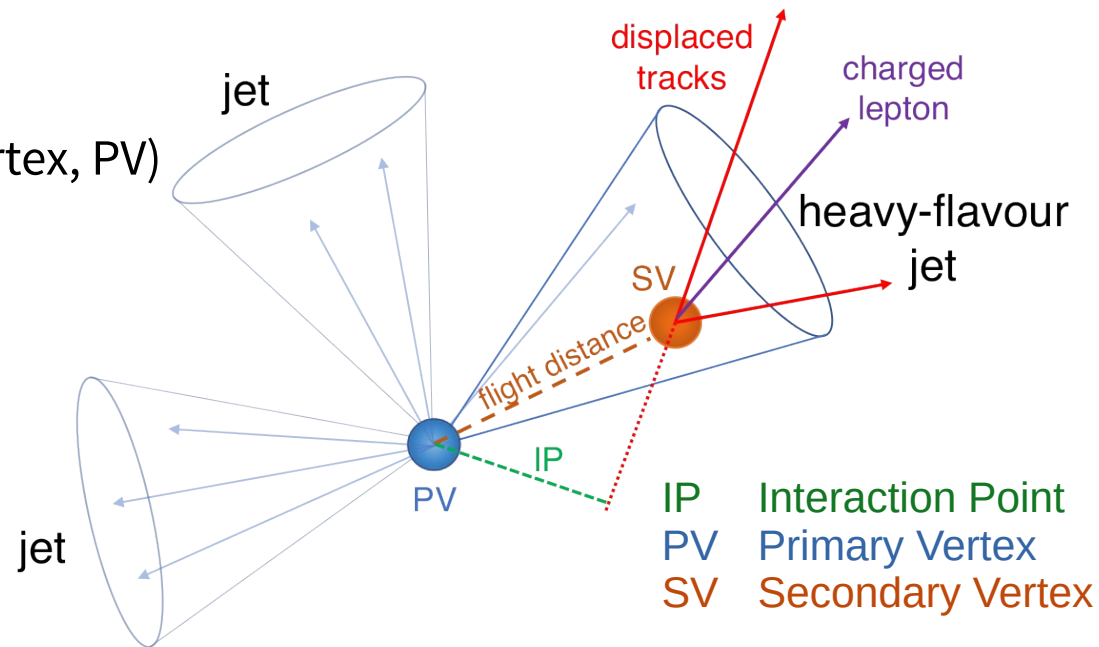
Run Number: 266904, Event Number: 25884805

Date: 2015-06-03 13:41:54 CEST



Secondary Vertex Reconstruction

- Not all particles decay immediately
 - Produced at collision (primary vertex, PV)
 - Propagation during finite lifetime
 - Decay → secondary vertex (SV)
- Lifetime of b-quarks: $\mathcal{O}(10^{-12} \text{ s})$
 - Flight distance: $\mathcal{O}(100 \text{ } \mu\text{m})$
 - Can be resolved with modern tracking detectors



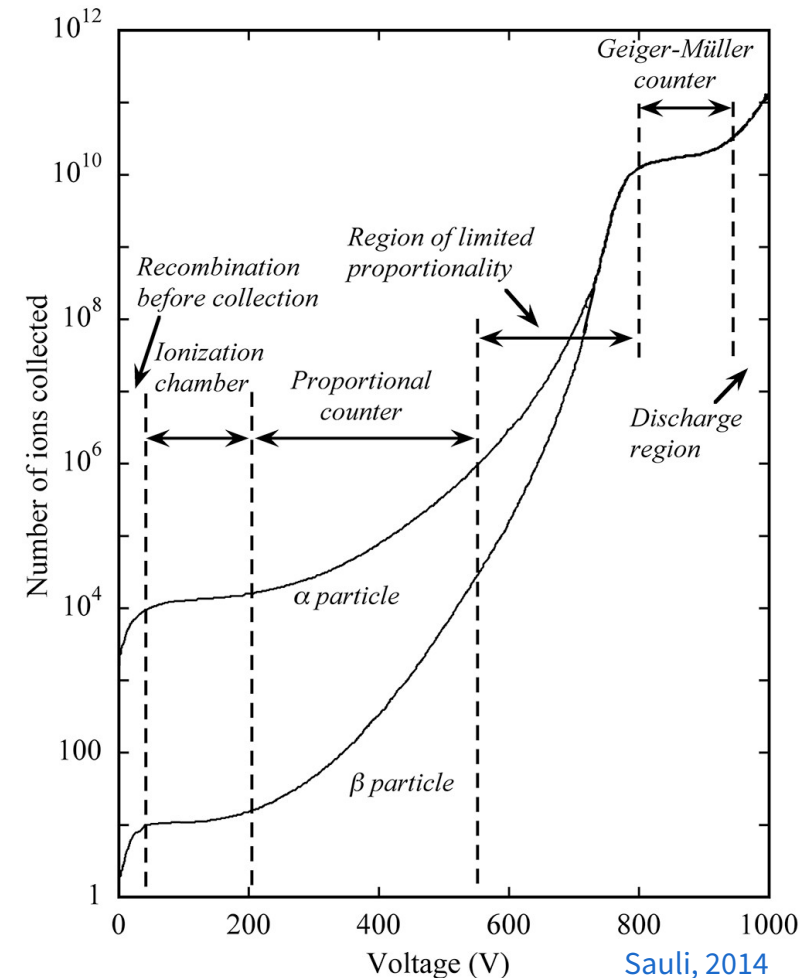
- Indication of SV hints at b-quarks, used for e.g. b-Tagging
 - Important top quarks decays
 - Lifetime of b-mesons $\tau \approx 10^{-12} \text{ s} \rightarrow d/\gamma \approx 0.1 \text{ mm}$

Gaseous Detectors

Primary & secondary ionization of gas atoms

Gaseous Detectors: Operating Principle

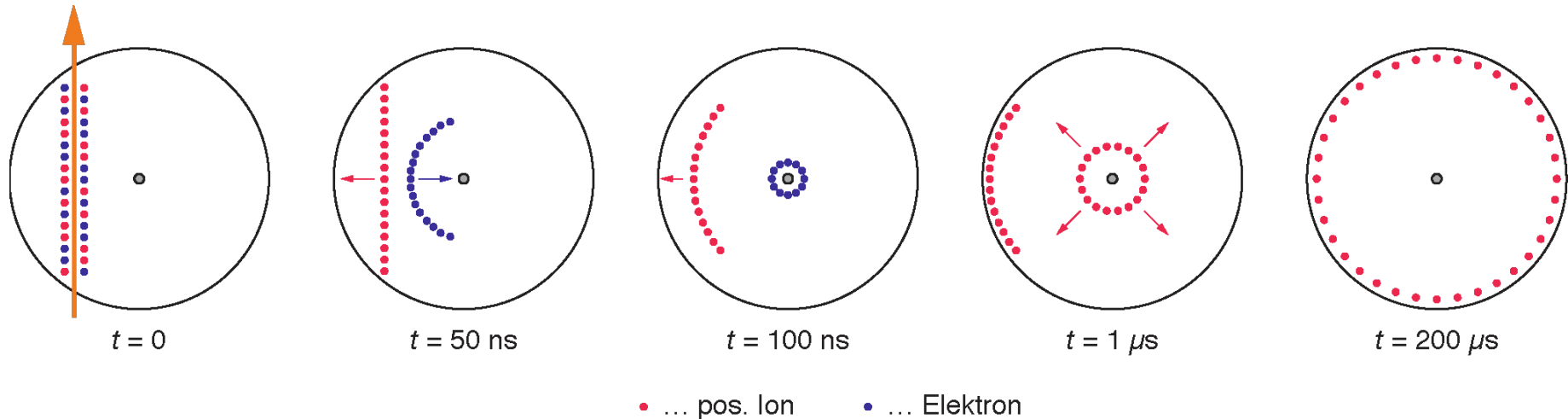
- **Primary signal:** charged particle generates electron-ion pairs by ionization
 - Noble gases: relatively low ionization energy
 - Average energy to generate a pair ~ 30 eV
 - Number proportional to deposited energy
- **Amplification:** different working ranges depending on applied voltage
 - Medium voltages: proportional amplification
 - High voltages: Avalanche formation due to secondary ionizations



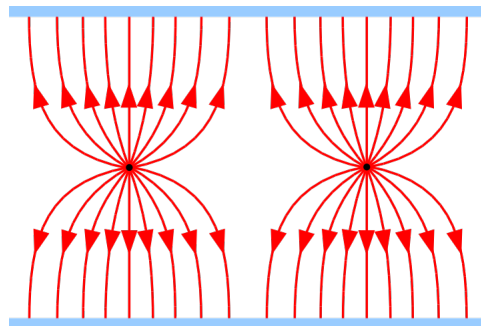
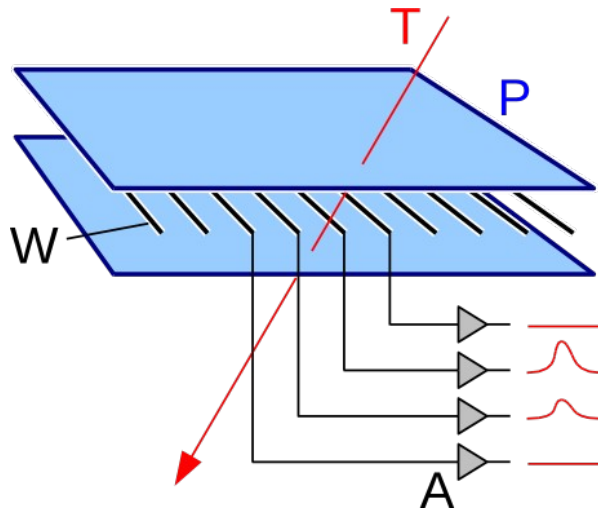
Sauli, 2014

Proportional Counter

- Very similar to the Geiger counter: anode in the form of thin wire
- High field near wire leads to electron multiplication / signal amplification
- Choice of voltage: proportional range
 - Output signal proportional to original number of ionizations



Multi Wire Proportional Chamber (MWPC)

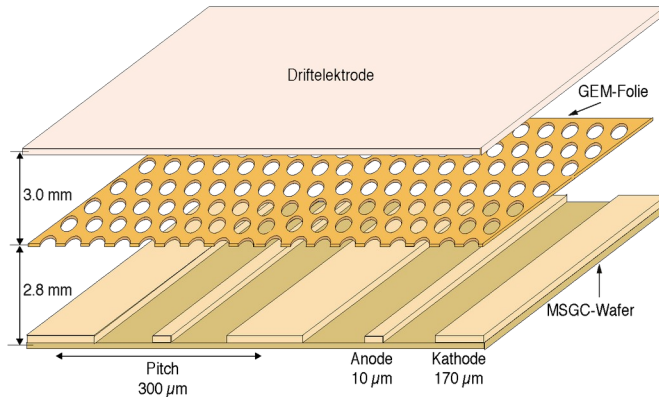


- Essentially many proportional counters next to each other, without separating walls
- Wires spaced a few millimeters apart
 - Good spatial resolution of a traversing particle
 - Large areas possible
 - Electronic selection
- High rates possible: 1000 particles/s
for comparison, bubble chamber: 1-2 particles/s
- Nobel Prize 1992 for Georges Charpak



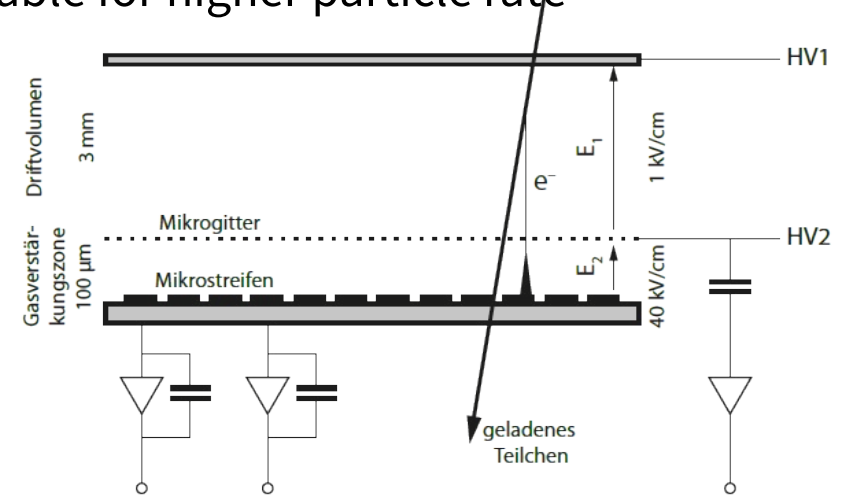
Micropattern Gas Detectors

- Replacement of fragile wires by micro structures
- Potentially better spatial resolution and applicable for higher particle rate



Gas Electron Multiplier (GEM)

- Perforated, metallized Kapton foil, High voltage between electrodes
- Strong dipole field in perforation holes: Gas amplification

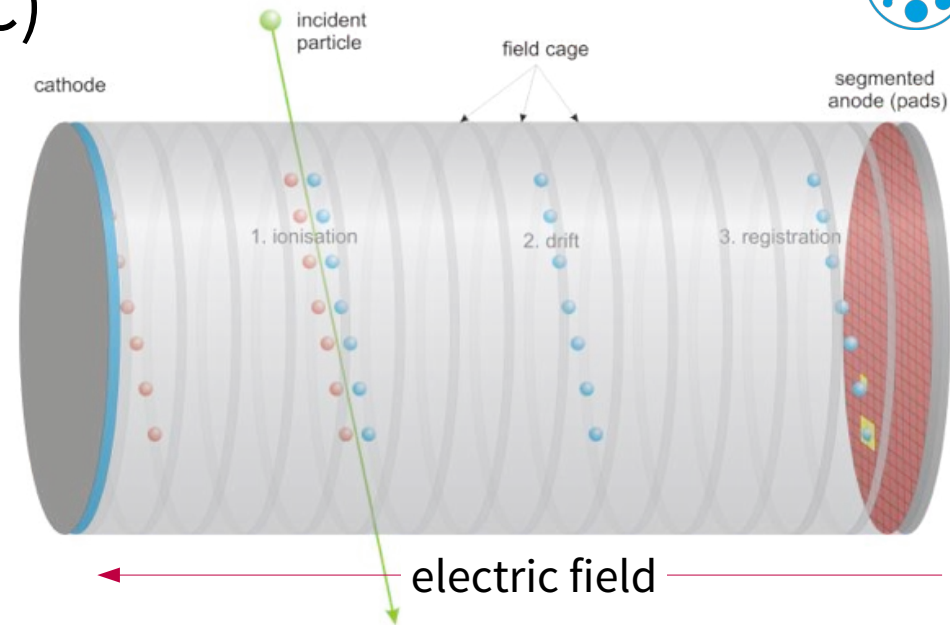


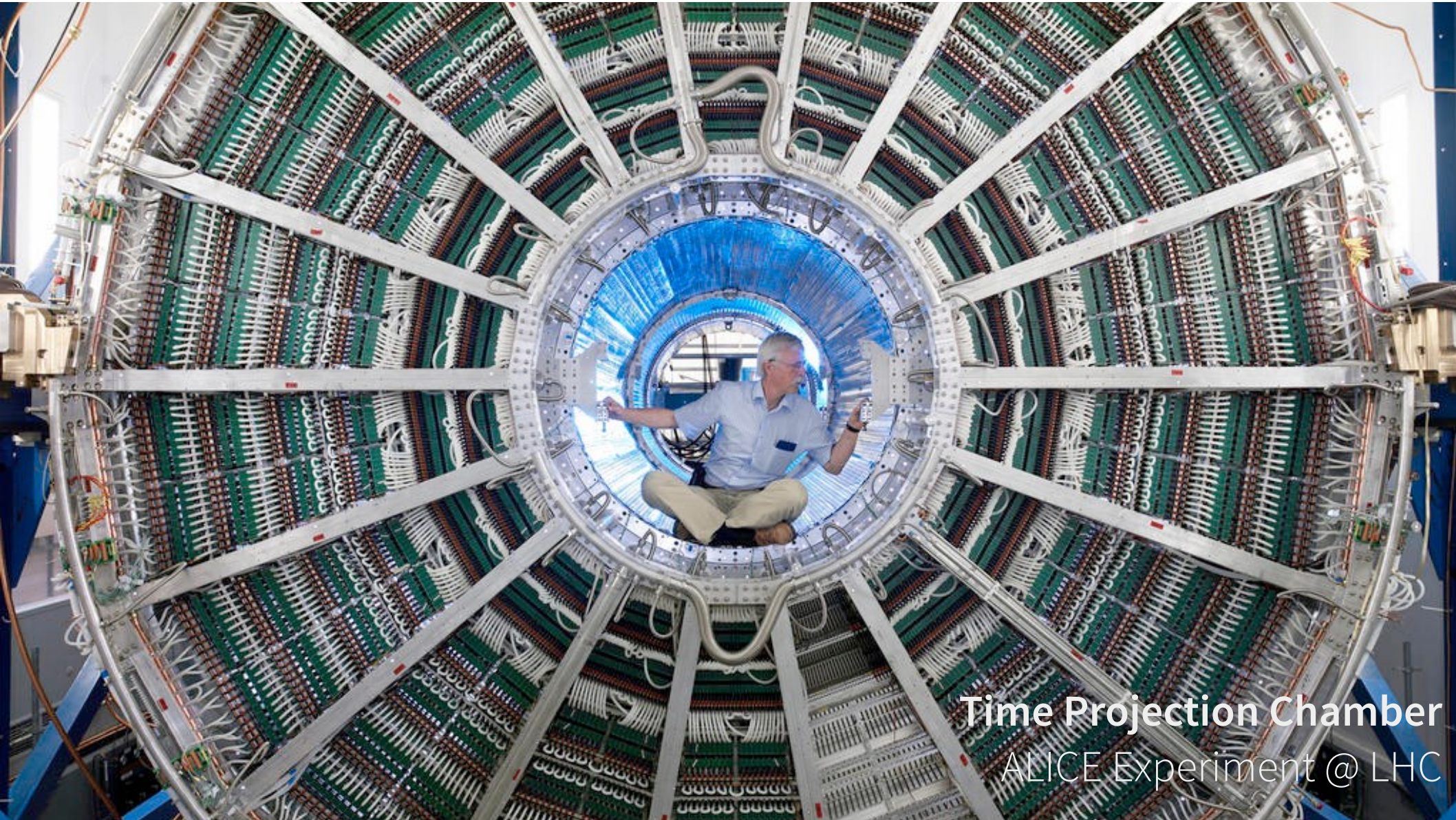
Micro-Mesh Gas Detectors (Micromegas)

- Metallic micro-grid
- Electron avalanche evolution near the lattice: Gas amplification

Time Projection Chambers (TPC)

- Large gas detector system
- Ionization along the particle track
 - Electrons and ions drifting in the E-field
 - Segmented anode: 2D information
 - Measurement of drift time: 3D information
- Readout at anode side e.g. via multi-wire proportional chamber, GEMs, ...

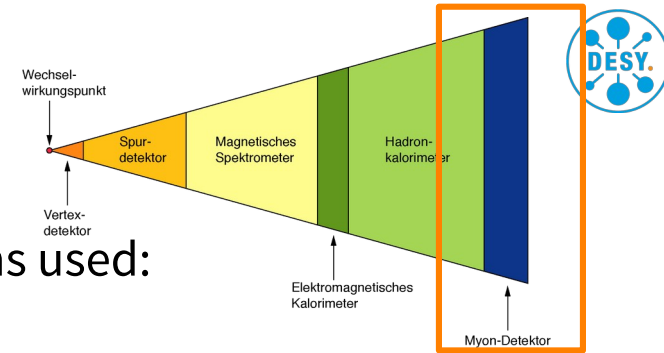




Time Projection Chamber
ALICE Experiment @ LHC

Muon Spectrometers

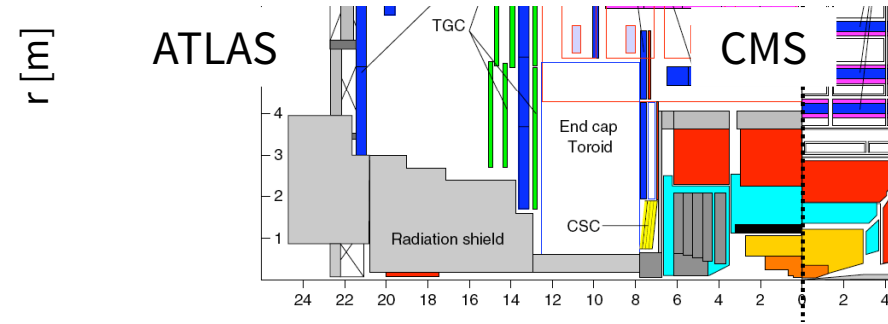
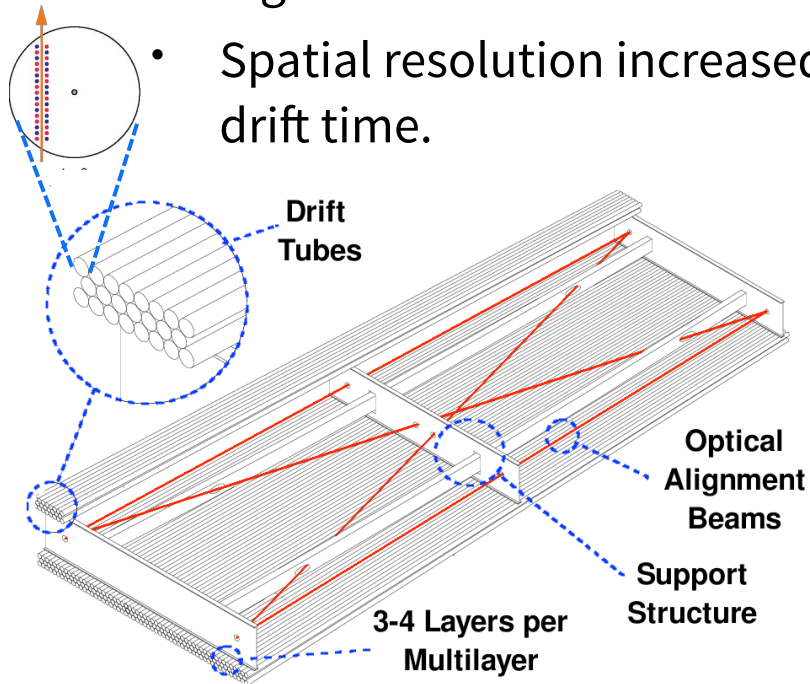
- Identification and precise momentum measurement of muons outside of the magnet – often gas detector systems used:
 - Requires huge areas to be instrumented
 - Position resolution is not extremely demanding
- Typical track in Muon System: ~ 20 hits
- Very often two possibilities for muon tracking:
 - *Standalone* – purely based on muon system
 - *Combined* – use info from inner detectors & muon system
- Standalone capabilities can be crucial at high luminosities
- The momentum measurement is dominated by
 - Inner detectors @ low p_T
 - Muon system @ high p_T



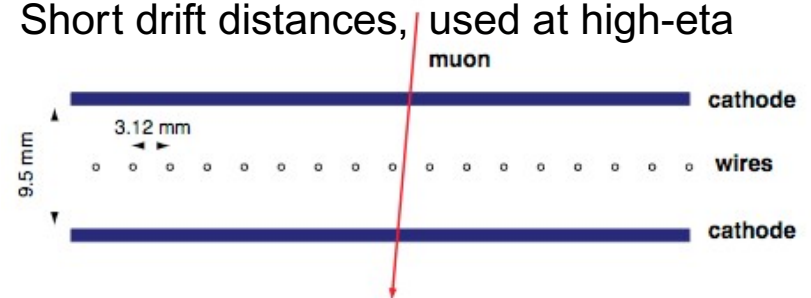
ATLAS

Muon Systems @ LHC

- Monitored Drift Tubes (MDT)
 - Gas-filled drift tubes with central wire
 - Signal read out on both ends
 - Spatial resolution increased by recording drift time.

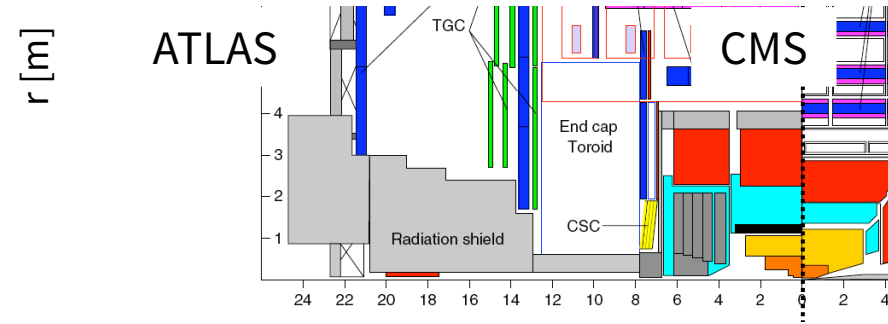
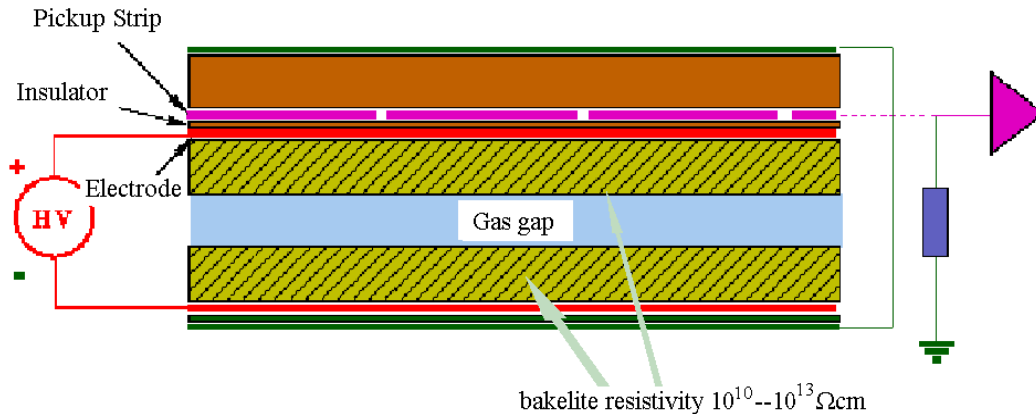


- Cathode Strip Chambers (CSC)
 - Array of anode wires crossed with copper cathode strips
 - Short drift distances, used at high-eta

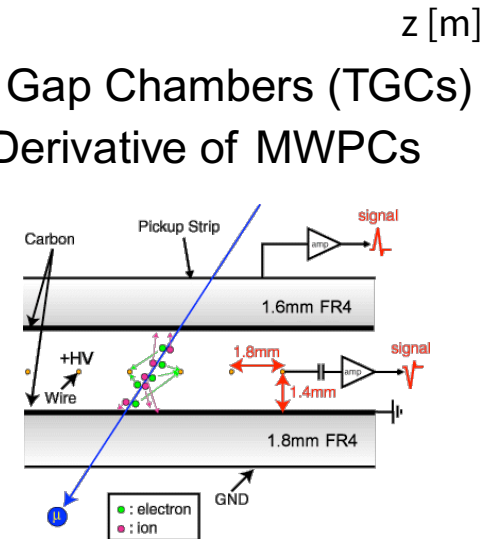


Muon Systems @ LHC (II)

- Resistive Plate Chambers (RPCs)
 - Parallel plate electrodes with HV leads to uniform electric field in the gas gap
 - Charge carriers drift towards anode, generate avalanche in high electric field
 - Large number of charge carriers induces a signal on a read out electrodes



- Thin Gap Chambers (TGCs)
 - Derivative of MWPCs

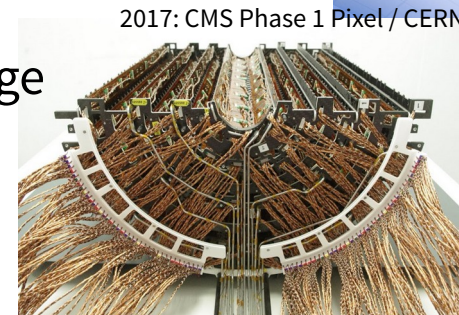
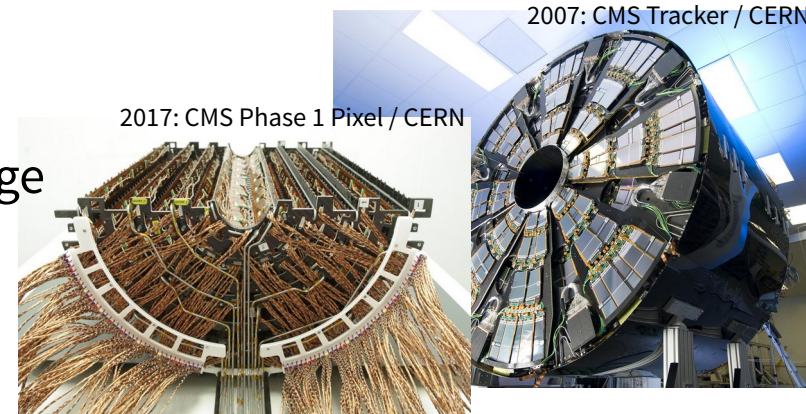
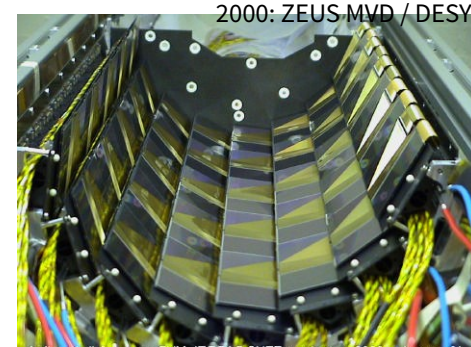
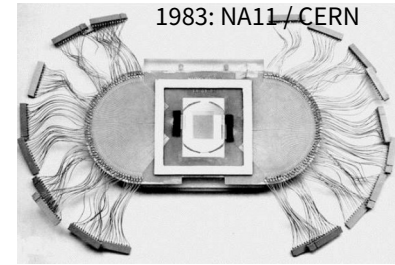


Semiconductor Detectors

Across the band gap into the conduction band

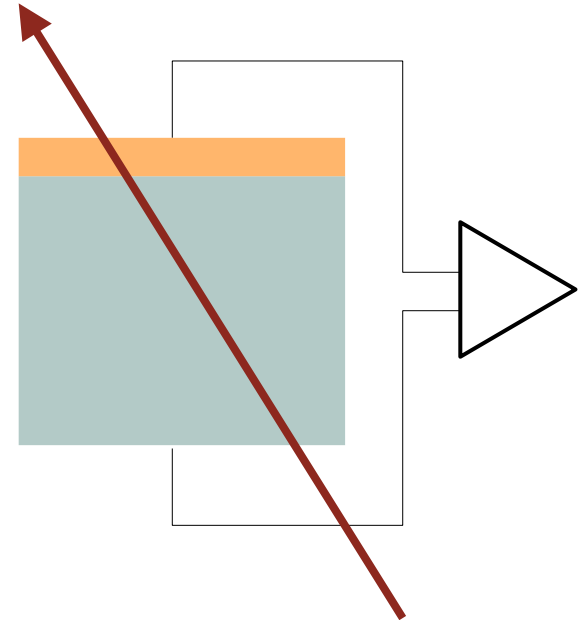
Silicon Tracking Detectors in Particle Physics

- Silicon tracking detectors have long history in particle physics
- Instrumental in discovery of Higgs boson at LHC
- Large detectors installed in ATLAS & CMS
 - Tracking detectors: strips, 200 m² silicon, 70M channels
 - Vertex detectors: pixels, 1 m² silicon, 140M channels
- Detector upgrades for HL-LHC in preparation
 - More resilient against radiation-induced damage
 - Additional capabilities (e.g. triggering)



Detection Principle

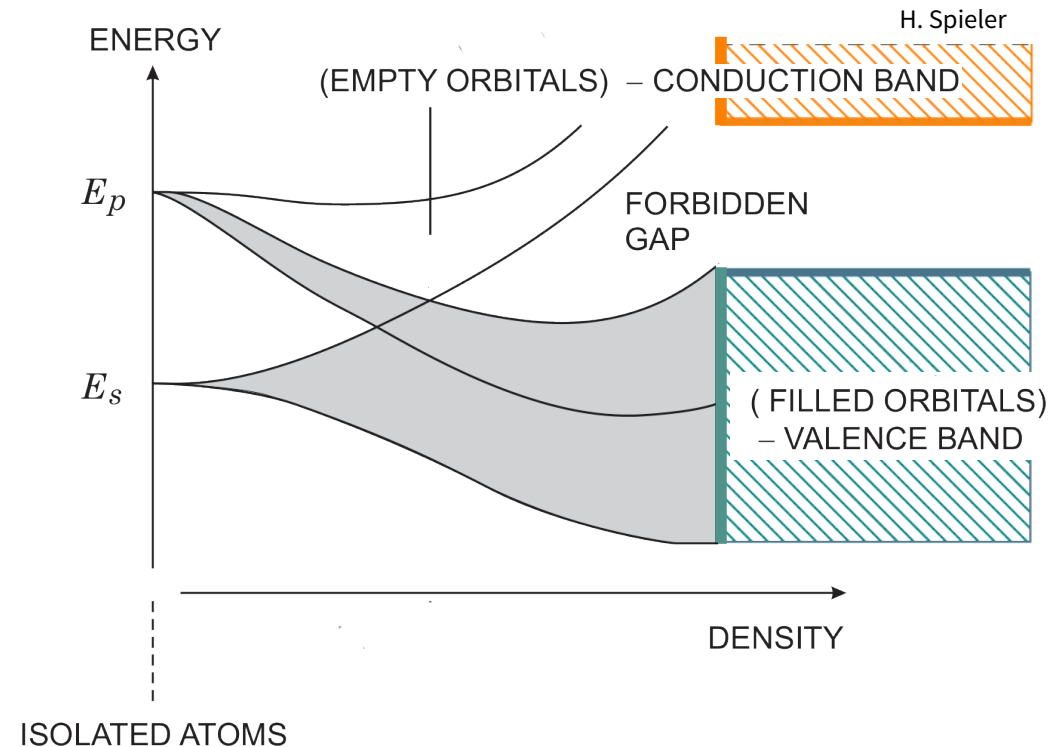
- Solid state detector
 - Many higher density than gas detectors
 - High energy loss over relatively short distance
- Operating principle analogous to gas detectors
 - "Ionization" to generate free charge carriers
 - Drift due to electric field
 - Detection as electrical signal at electrodes
- Semiconductors:
Silicon, Diamond, Germanium, GaAs, CdTe, ...



We will use many analogies to gas detectors...

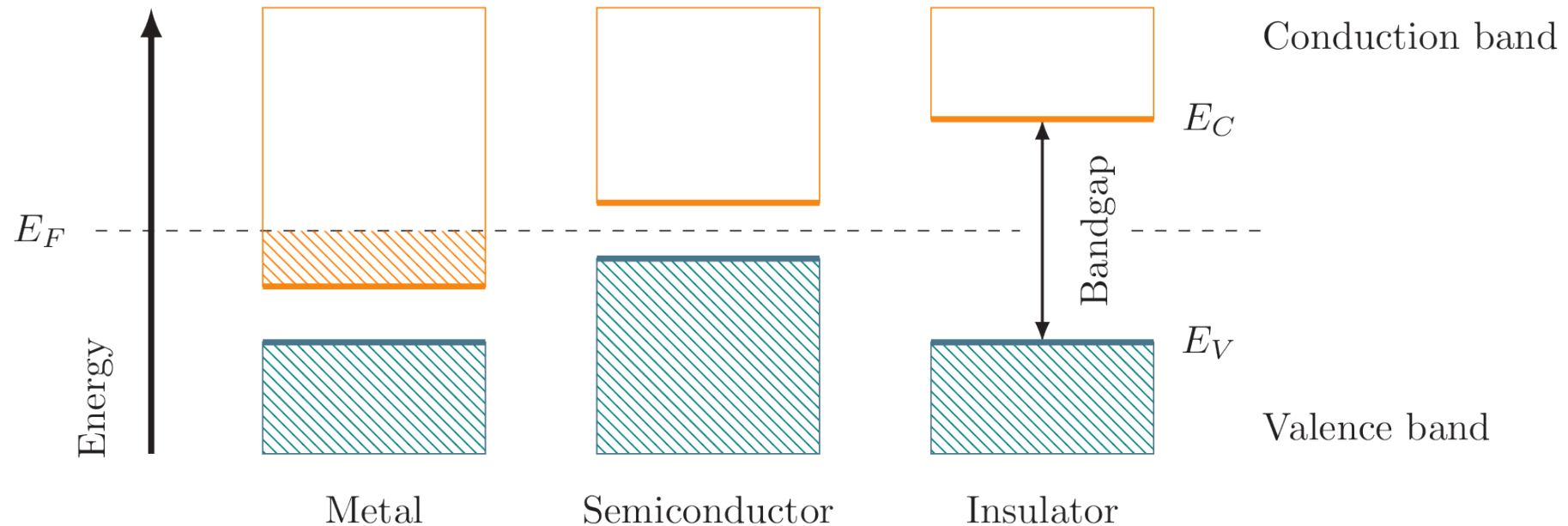
Band Model

- Atom: discrete energy levels, orbitals
- Crystal lattice: energy levels blur into energy bands
- Formation of energy bands
 - Valence band – (last) fully filled
 - Band gap
 - Conduction band



Band Model: Insulator - Semiconductor - Conductor

- Position of valence and conduction band determines conduction property:



Choice of the Semiconductor

- Semiconductor detectors in high-energy physics: almost exclusively **silicon**
 - Industrially available via industry (availability, further development)
 - Band gap large enough $E_G = 1.12 \text{ eV}$ for operation at room temperature
 - Average energy for electron-hole generation: $E = 3.64 \text{ eV}$ (gas detector: x 10)
- Germanium: $E_G = 0.74 \text{ eV}$
 - Too many free charge carriers at room temperature, needs cooling
 - Better energy resolution, often used in spectrometers
- Diamond: $E_G = 5.4 \text{ eV}$, sometimes used for special radiation hardness requirements
- GaAs, CdTe, CYT... : mainly used in X-ray spectroscopy

Detecting a Particle with Intrinsic Silicon

- Silicon sensor: $A = 1 \text{ cm}^2$ and $d = 300 \mu\text{m}$
- Signal of MIP:
 - Mean ionization: $E_0 = 3.6 \text{ eV (silicon)}$
 - Mean energy loss: $dE/dx = 3.9 \text{ MeV/cm}$

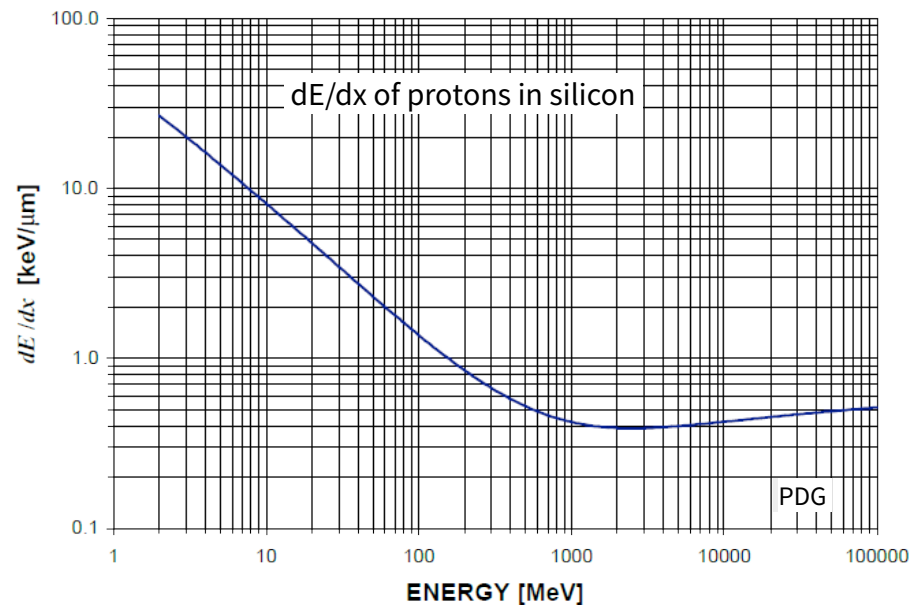
$$\frac{dE}{dx} \cdot \frac{d}{E_0} = 3.9 \cdot 10^6 \text{ eV/cm} \cdot 0.03 \text{ cm} / 3.6 \text{ eV}$$

$$\approx 3 \cdot 10^4 \text{ e/h pairs}$$

- Thermally excited charge carriers in silicon: $n_i = 1.45 \times 10^{10} \text{ cm}^{-3}$ (at 300K)

$$n_i \cdot d \cdot A = 1.45 \cdot 10^{10} \text{ cm}^{-3} \cdot 0.03 \text{ cm} \cdot 1 \text{ cm}^2$$

$$\approx 4 \cdot 10^8 \text{ e/h pairs}$$



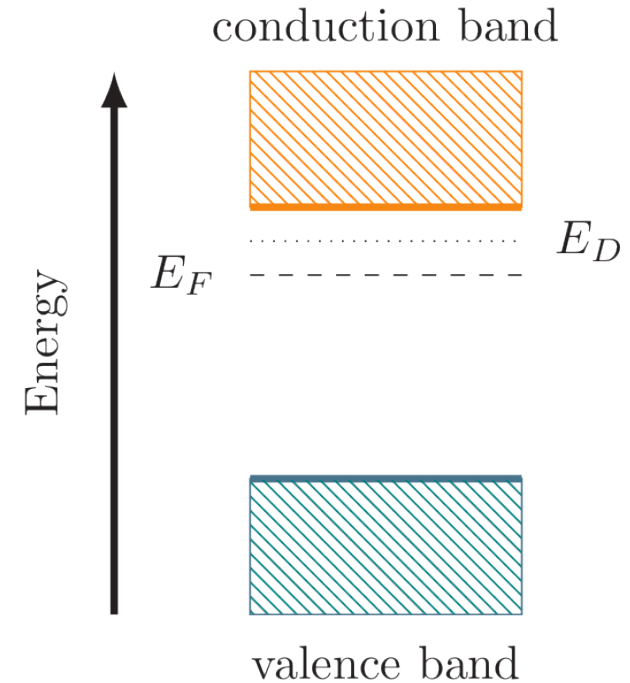
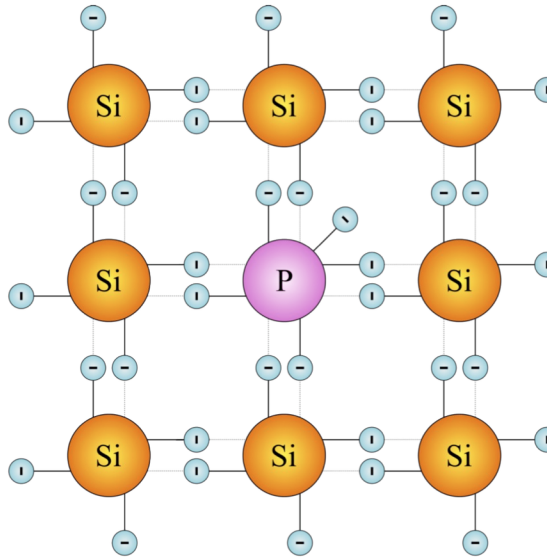
density silicon:
 $N \approx 10^{22} \text{ atoms/cm}^3$

Doping Silicon – *n*-type

typical doping (*p-in-n* sensor):
 $N_D \approx 10^{12} \text{ cm}^{-3}$



- Adding group-V element (phosphorus, arsenic)
- Four covalent bonds, one “dangling” e
- Introduces “donor” state
- Negative majority charge carrier: “*n*”

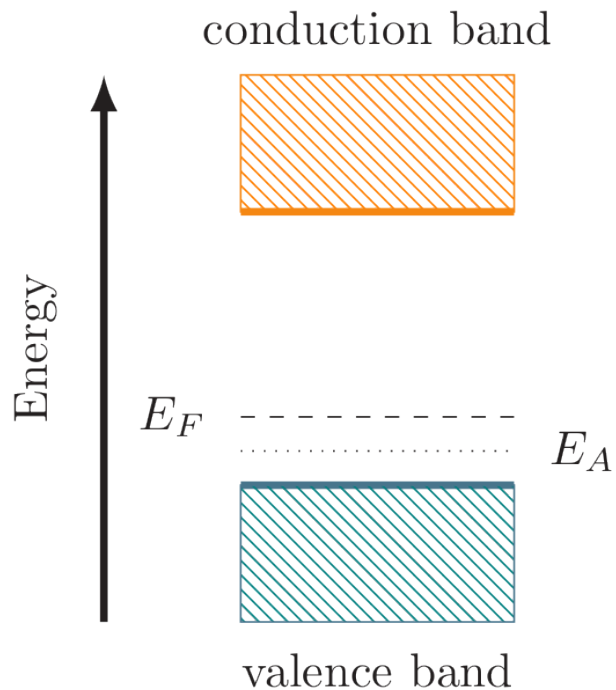
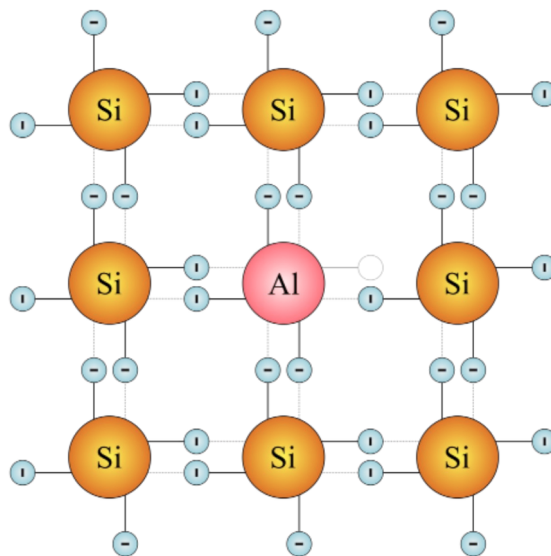


Doping Silicon – *p*-type

typical doping (*p*-in-*n* sensor):
 $N_A \approx 10^{15} \text{ cm}^{-3}$

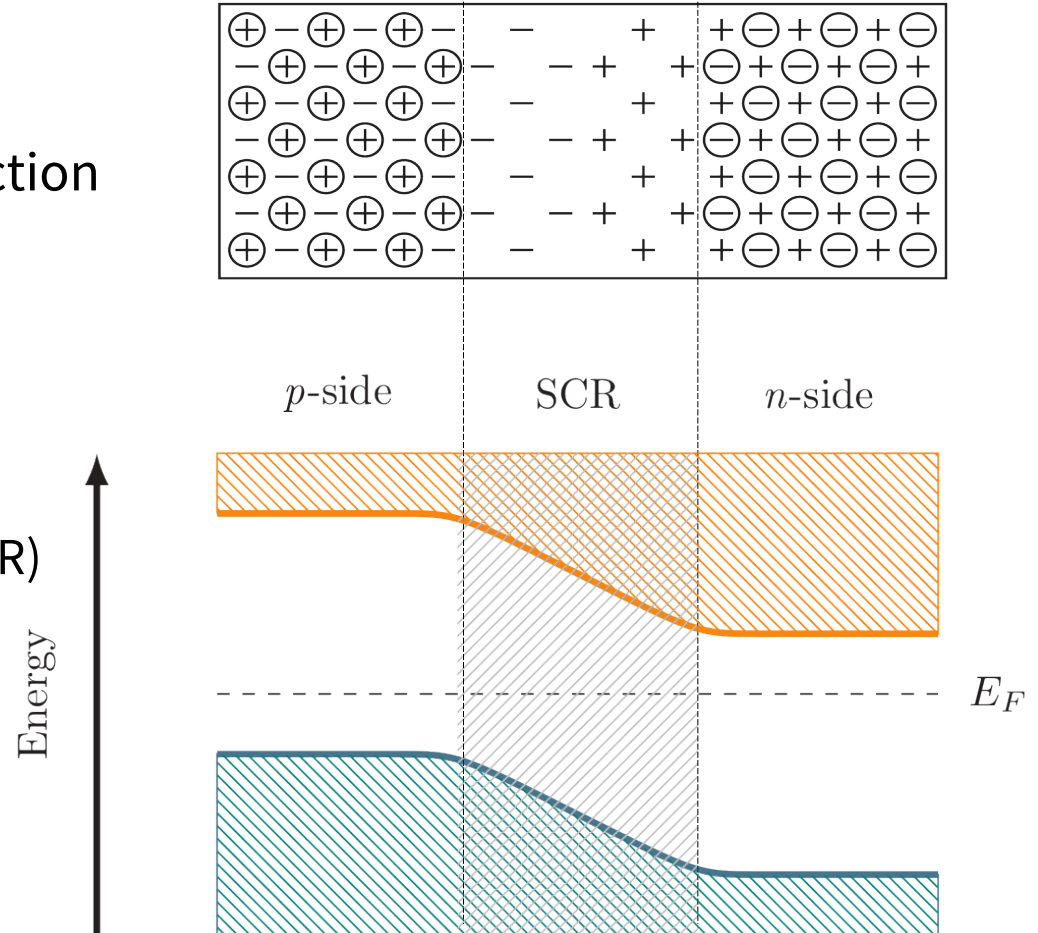


- Adding group-III element (boron, aluminum)
- Vacancy in covalent bonds – “hole”
- Introduces “acceptor” state
- Positive majority charge carrier: “*p*”



Forming a pn -Junction

- Electrons and holes diffuse over junction
- Constant Fermi level:
Deformation of energy bands
- Donor/acceptor atoms remain
 - Depleted / space charge region (SCR)
 - Potential U_{bi} builds up
- Thermal equilibrium:
Built-in potential balances diffusion



Built-in Voltage U_{bi}



silicon *p-in-n* sensor:

$$N_A \approx 10^{15} \text{ cm}^{-3}$$

$$N_D \approx 10^{12} \text{ cm}^{-3}$$

$$k_B T \approx 0.026 \text{ V}$$

$$n_i = 1.45 \times 10^{10} \text{ cm}^{-3}$$

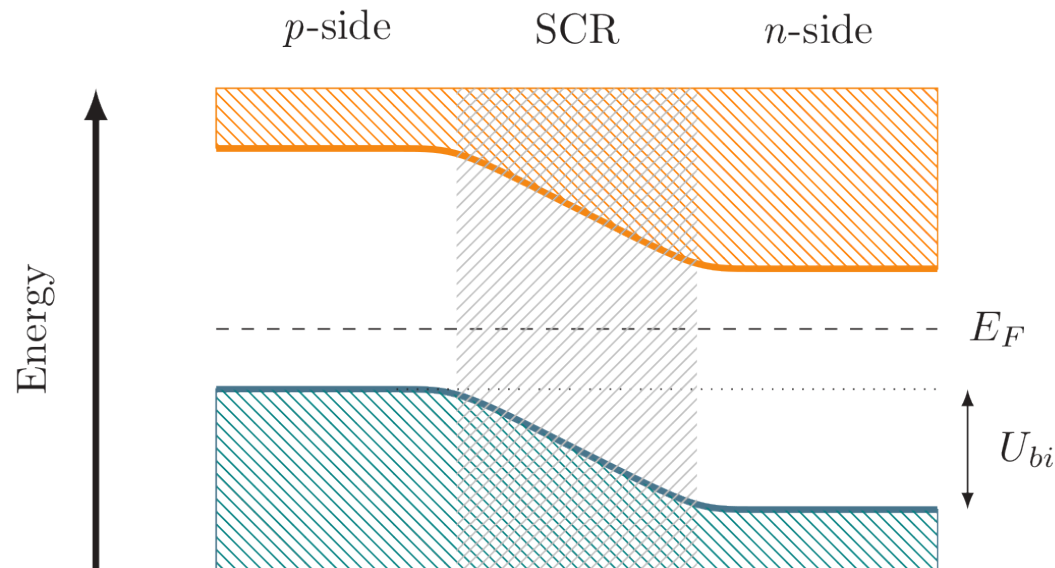
- Potential across the junction: $U_{bi} = E_{Fn} - E_{Fp}$
 difference of Fermi energies
p-in-n sensor: $U_{bi} \approx 0.4 \text{ V}$

$$= k_B T \ln \left(\frac{N_A N_D}{n_i^2} \right)$$

- Thickness of built-in SCR:

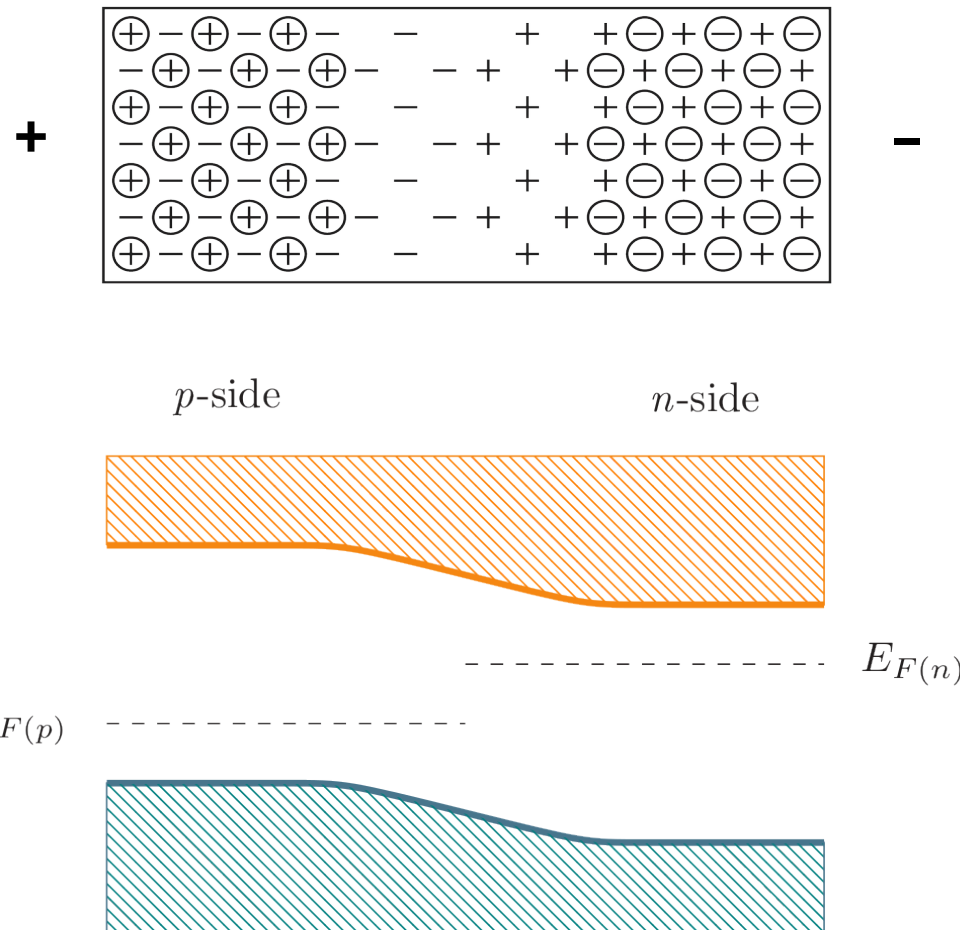
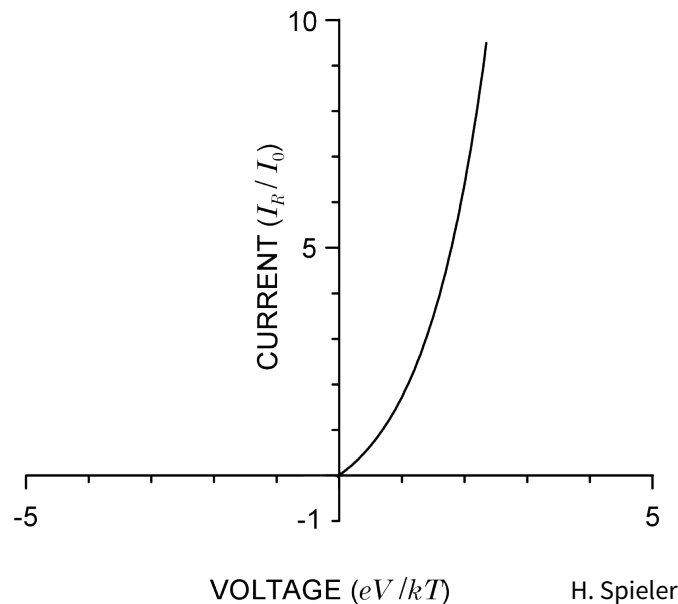
$$d(U_{bi}) = \sqrt{\frac{2 \epsilon_r \epsilon_0}{|N_D - N_A|} \cdot U_{bi}}$$

p-in-n sensor: $d \approx 20 \mu\text{m}$



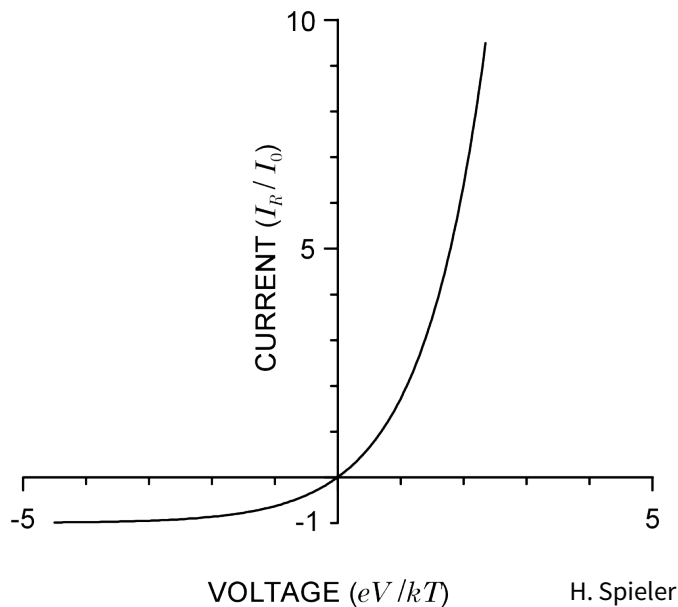
pn -Junction in Forward Bias

- Lowering potential difference
- Increases flow of electrons & holes
- Shockley eq. $I = I_0 (e^{eU/k_B T} - 1)$

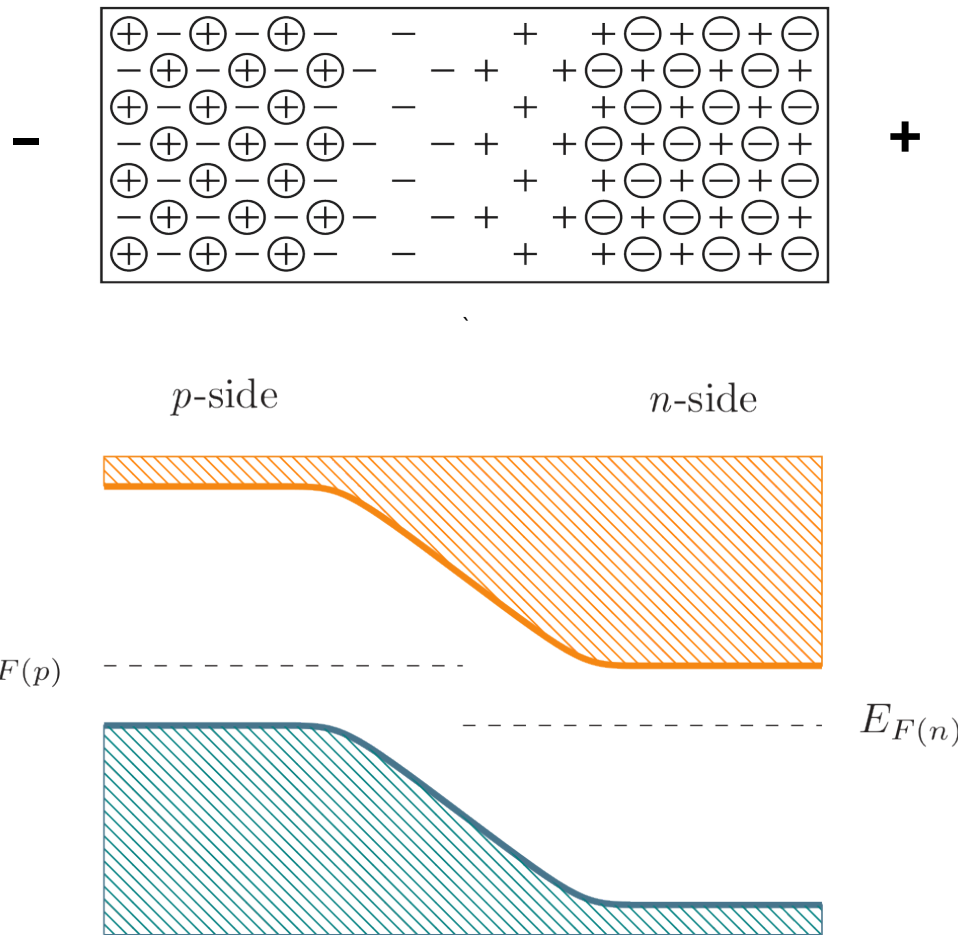


pn -Junction in Reverse Bias

- Raising potential difference
- Widens depletion region
- Shockley eq. $I = I_0 (e^{eU/k_B T} - 1)$



H. Spieler



pn -Junction in a Sensor

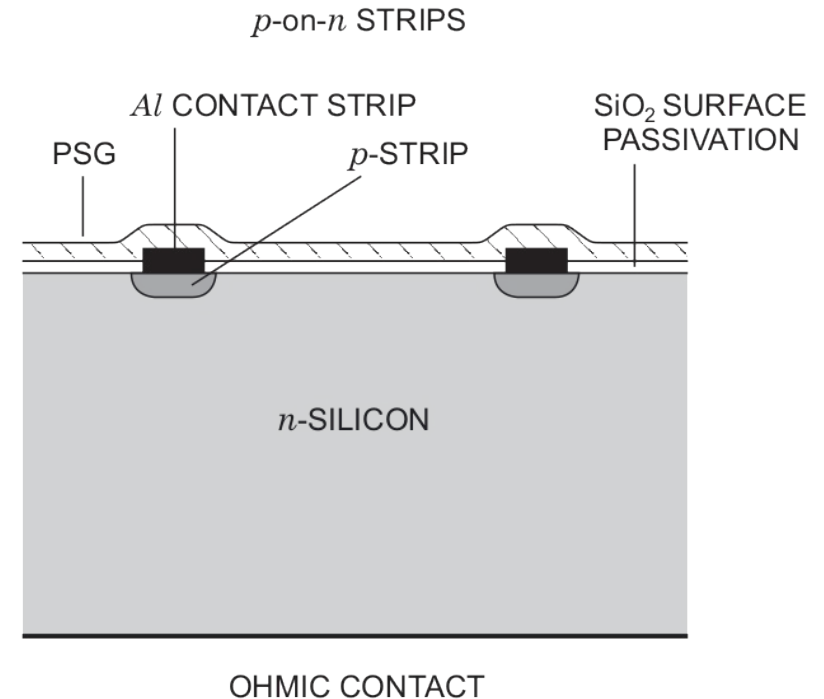


typical doping (p -in- n):

$$N_A \approx 10^{15} \text{ cm}^{-3}$$

$$N_D \approx 10^{12} \text{ cm}^{-3}$$

- Asymmetric pn -junctions, here: p -in- n
- Lightly doped n bulk sensor material
- Thin, highly-doped p implant
- Segmentation of implant: separate channels
- Backside: layer of highly doped n^+ as ohmic contact



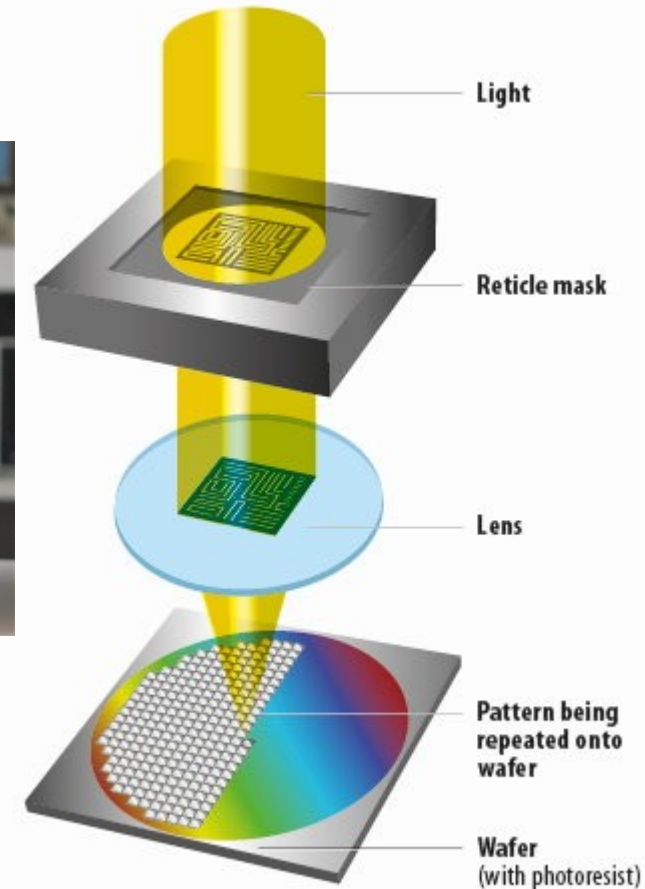
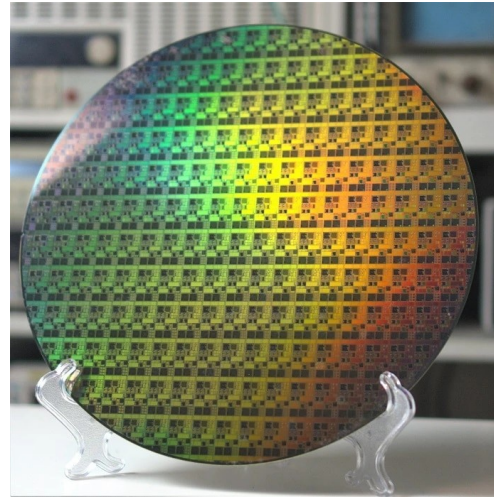
H. Spieler

Silicon Wafer Processing

- Patterning by selectively introducing impurities (dopants)

- Using photo lithography processes:

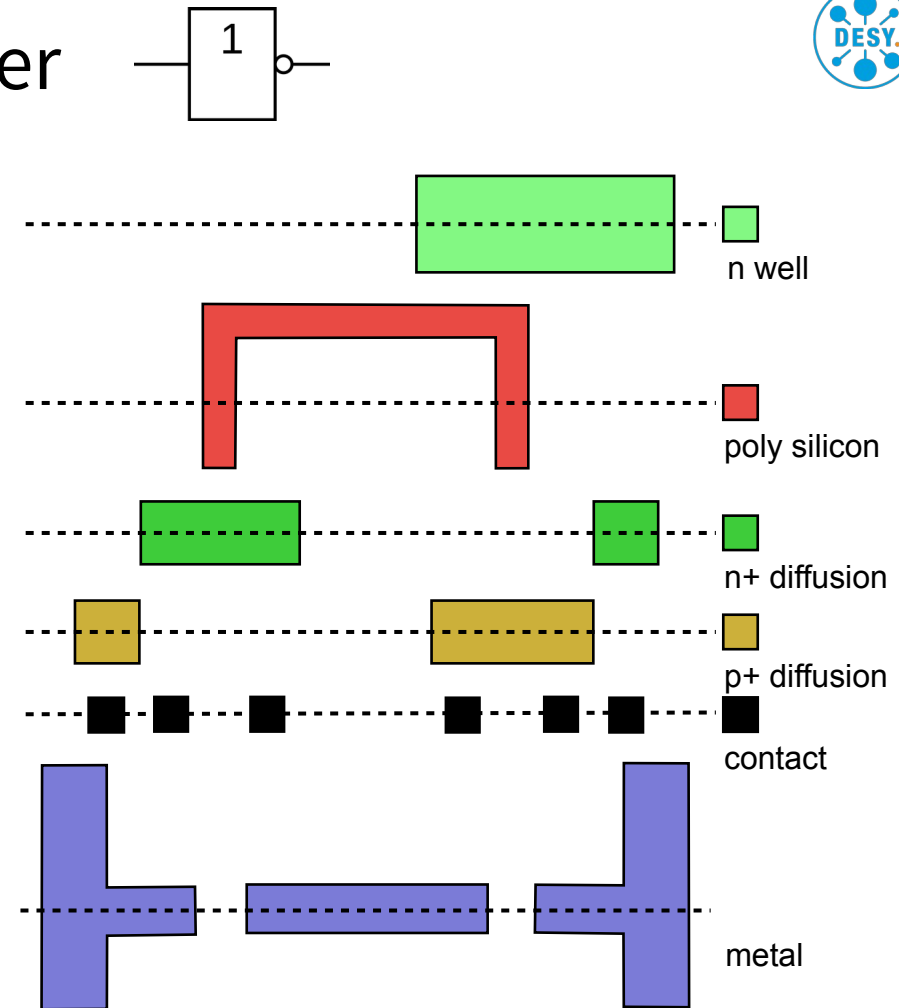
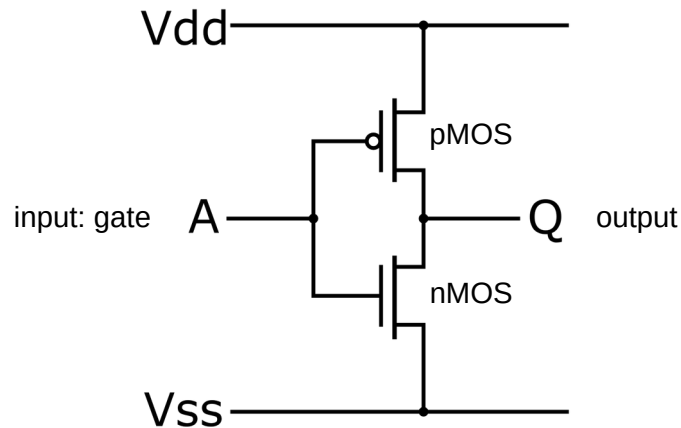
- Photoresist, etching, implantation
- Stepping due to limited reticle size



- Many steps involved in processing wafer, sensors: fewer, coarse structures; CMOS electronics: many more steps, fine structures

Example: Building a CMOS Inverter

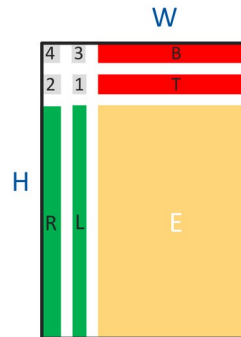
- Sensor electrodes, implants, transistors, traces are all defined via **masks**
 - Patterning of wafer surface for each type
- Example here: Inverter - requires 6 masks (and quite a few process steps...)
- Simplified representation of the process!



Reticles & Stitching

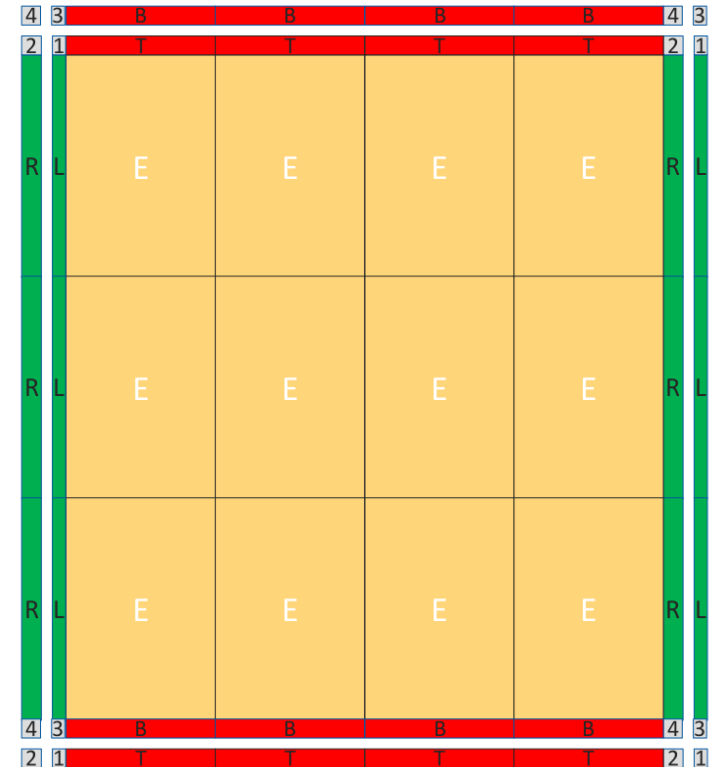
- Deep submicron processes:
Illumination area limited by photolithography
- Reticle
 - typically 2 cm x 3 cm
 - limits maximum size of chips
- Limitation can be overcome with stitching:

Design Reticle (typ. 2×3 cm)



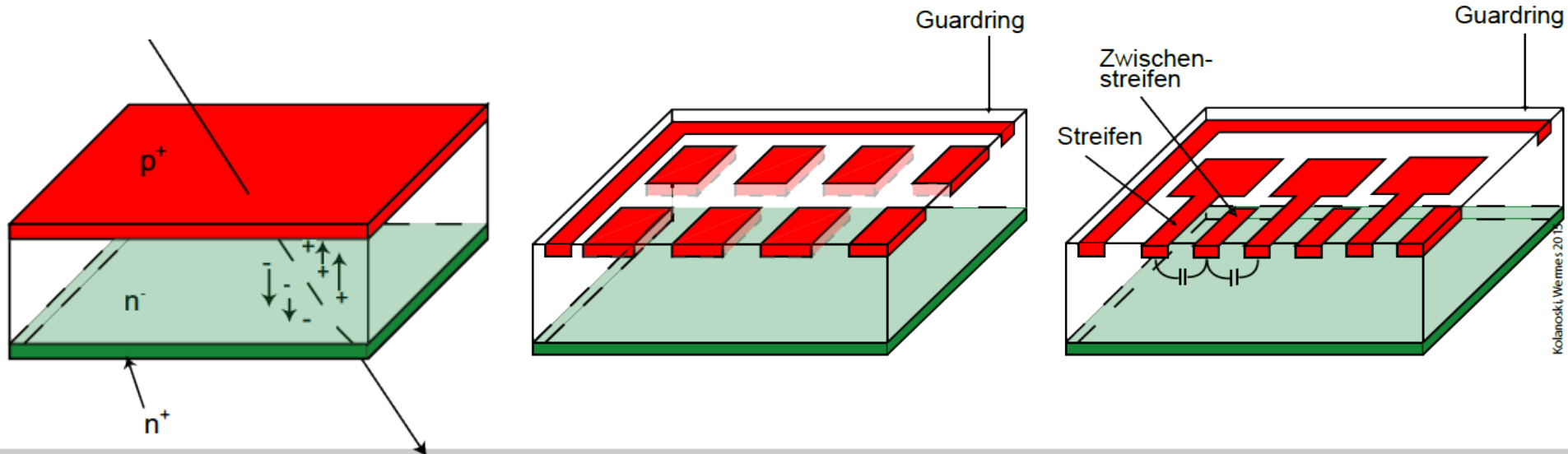
Circuits on wafer
 $n \times W$

$m \times H$



Segmentation of the Electrodes

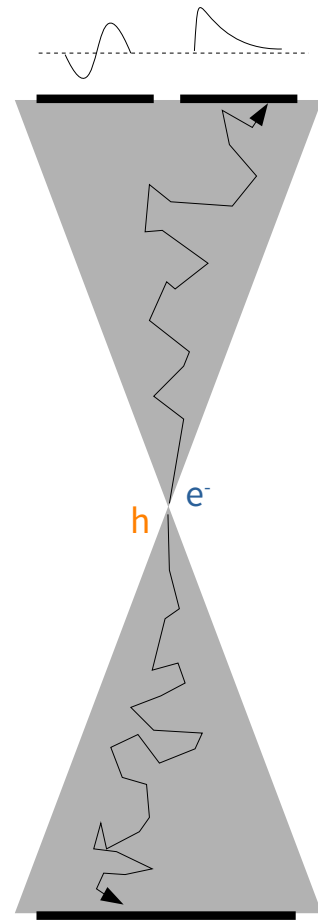
- Ionizing particle excites e- from valence band to conduction band during passage:
Generation of e/h pairs
- e/h pairs drift in electric field to electrodes, induce signal
- Segmentation of the electrode: very high spatial resolutions.
Small structures of a few 10 μm possible; experience from electronics industry



Signal Formation in Silicon Detectors

- Induced current by movement of charge carriers
- Diffusion
 - temperature-induced random motion, non-directional
 - Slow motion
- Drift
 - Directional motion due to electric field
 - Only in depleting areas
 - Fast motion
- Total motion: Superposition
- Best spatial resolution:
Interpolation of the signal between two electrodes:

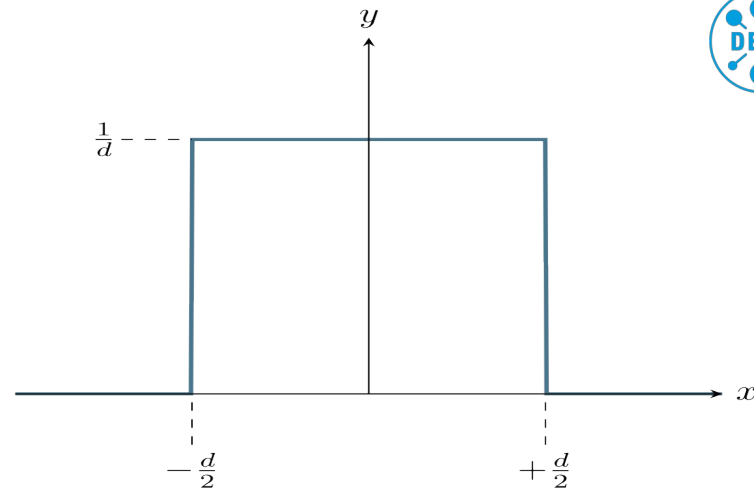
$$x = \frac{\sum_i Q_i x_i}{\sum_i Q_i}$$



Spatial Resolution

- The probability of particle crossing particular detector channel is uniformly distributed
- Normalized probability density function:

$$\int_{-\frac{d}{2}}^{\frac{d}{2}} f(x) dx = 1 \quad \rightarrow \quad f(x) = \frac{1}{d}$$



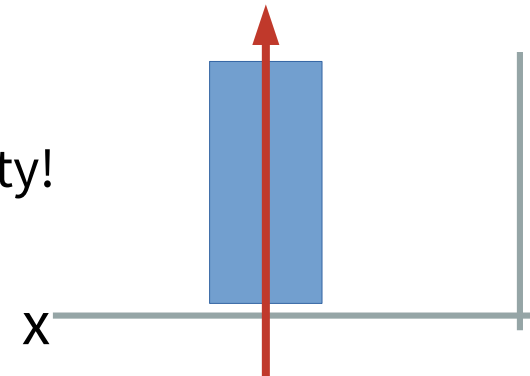
- Variance of position measurement:

$$\begin{aligned} \sigma_x^2 &= E[x^2] - \langle x \rangle^2 = \int_{-\frac{d}{2}}^{\frac{d}{2}} x^2 f(x) dx - \left(\int_{-\frac{d}{2}}^{\frac{d}{2}} x f(x) dx \right)^2 = \frac{1}{d} \int_{-\frac{d}{2}}^{\frac{d}{2}} x^2 dx - \left(\frac{1}{d} \int_{-\frac{d}{2}}^{\frac{d}{2}} x dx \right)^2 \\ &= \frac{1}{d} \frac{x^3}{3} \Big|_{-\frac{d}{2}}^{\frac{d}{2}} - \frac{1}{d^2} \frac{x^4}{4} \Big|_{-\frac{d}{2}}^{\frac{d}{2}} = \frac{d^2}{12} \end{aligned}$$

- **Uncertainty:** $\sigma_x = d/\sqrt{12}$

Spatial Resolution – Multiple Channels

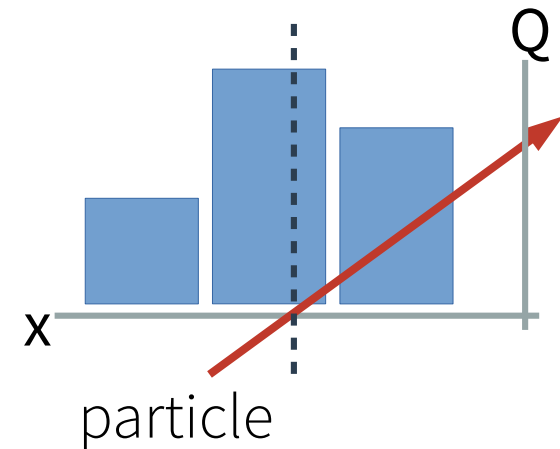
- Only approximation!
Many detectors provide better resolution than granularity!
- Just a single channel struck:
precision limited to variance of uniform distribution



$$x = x_i \quad \rightarrow \quad \sigma_x = d/\sqrt{12}$$

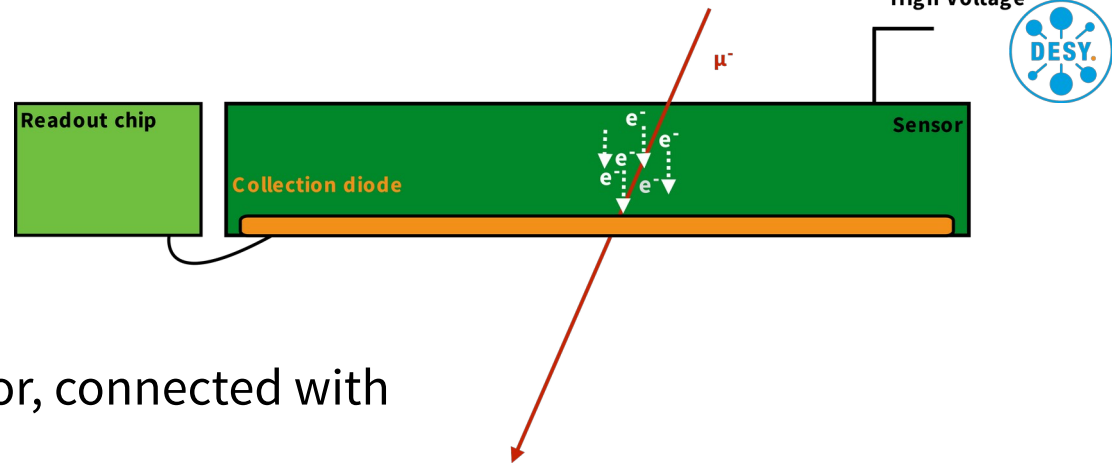
- Multiple channels struck (charge sharing):
interpolation using relative energy / charge distribution

$$x = \frac{\sum_{i=1}^N q_i x_i}{\sum_{i=1}^N q_i}$$

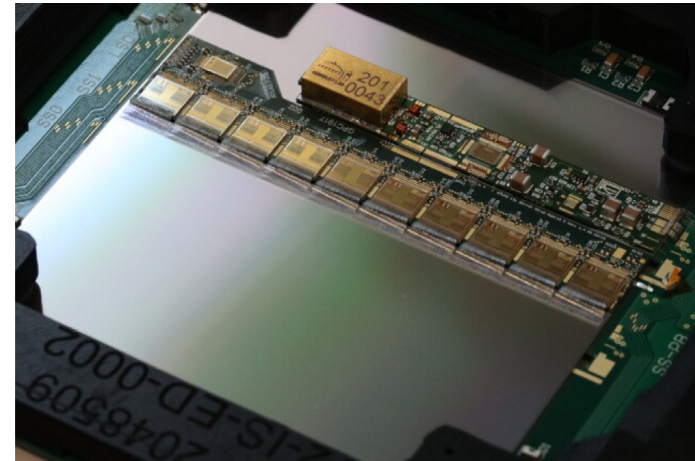


Strip Detectors

- Strips as readout electrodes
- Advantage:
 - Readout electronics next to sensor, connected with wirebonds,
 - Relatively easy to build, inexpensive, good for large areas
- Disadvantage:
 - Location measurement only along one coordinate
- Used for large areas:
Large radii from interaction point,
large lever arm for impulse measurement

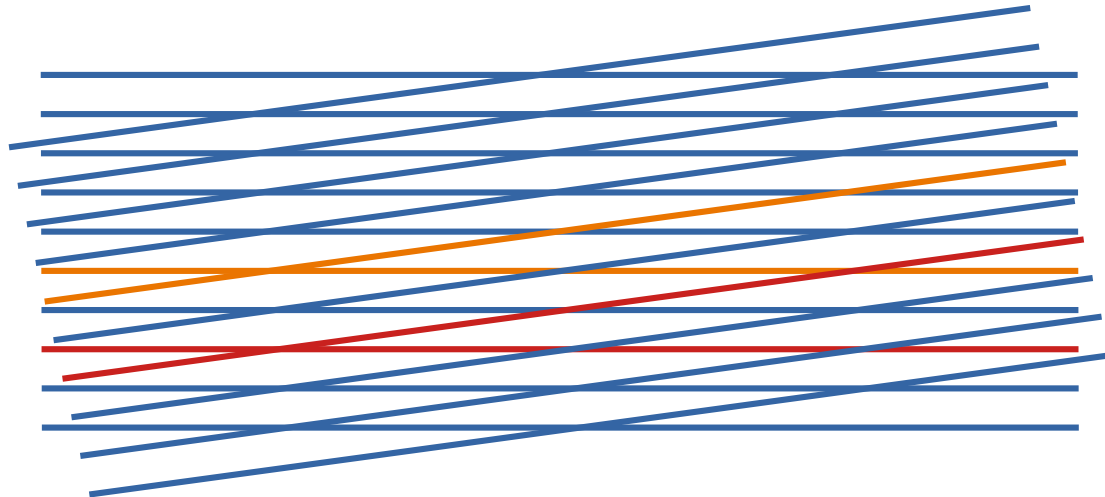


ATLAS ITk barrel long strip module prototype

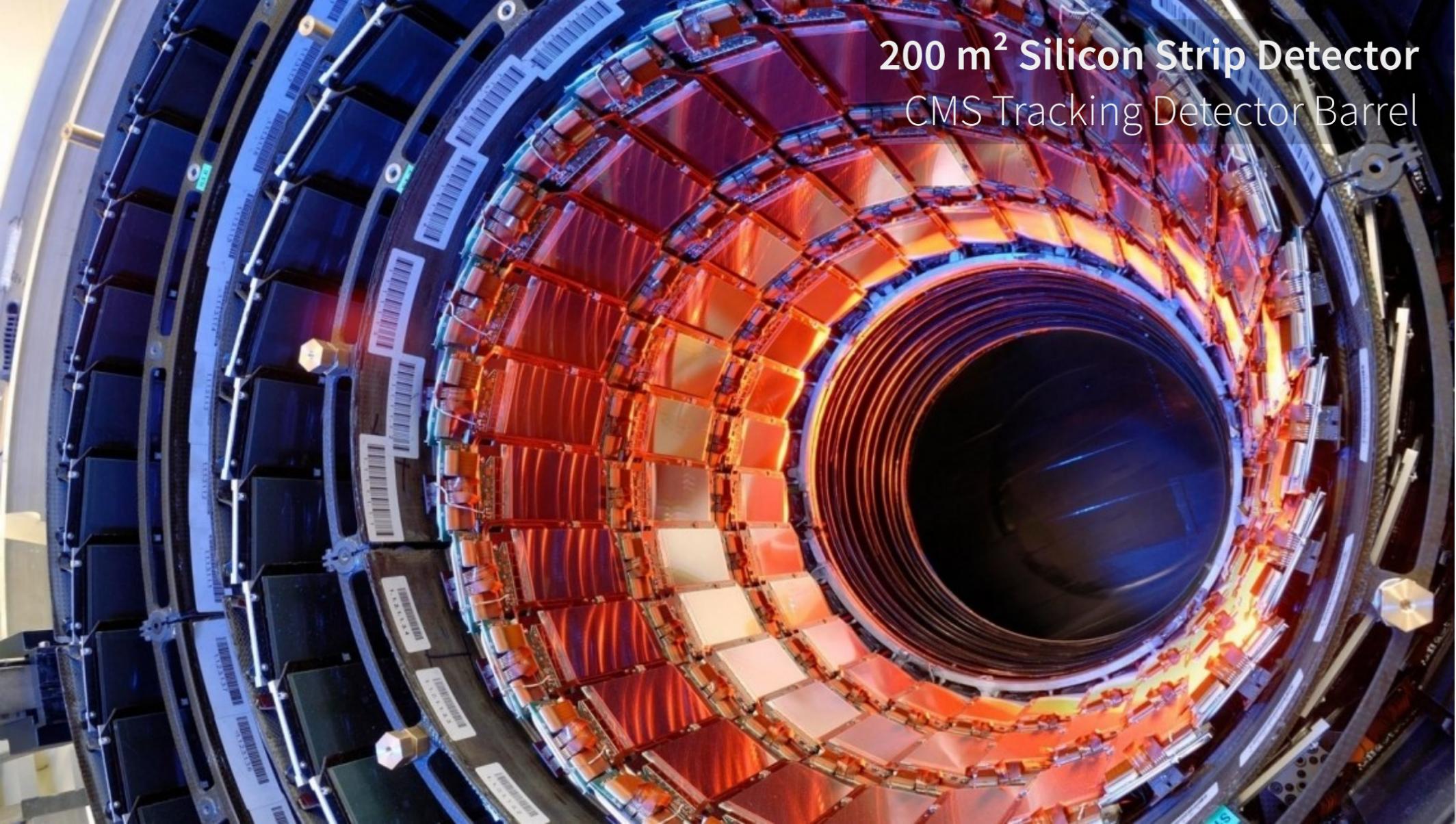


Strip Detector – Adding a 2nd Layer

- 2D measurement using stereo angle
 - Two detector modules on top of each other with a **small relative rotation angle**
 - Limit on total particle rate due to ambiguities:
- “Ghost Hits”
 - Appear with > 2 particles crossing the sensor
 - Impossible to distinguish particle crossing point from other strip coincidences



→ Reason for **small stereo angle!** Reduce number of other strips crossed

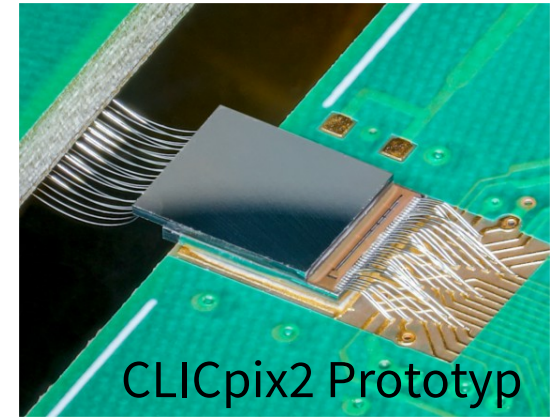


200 m² Silicon Strip Detector
CMS Tracking Detector Barrel

Silicon Pixel Detectors

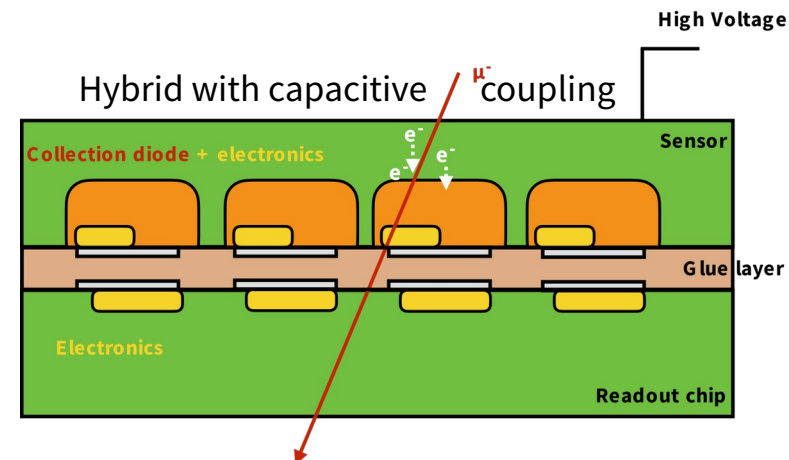
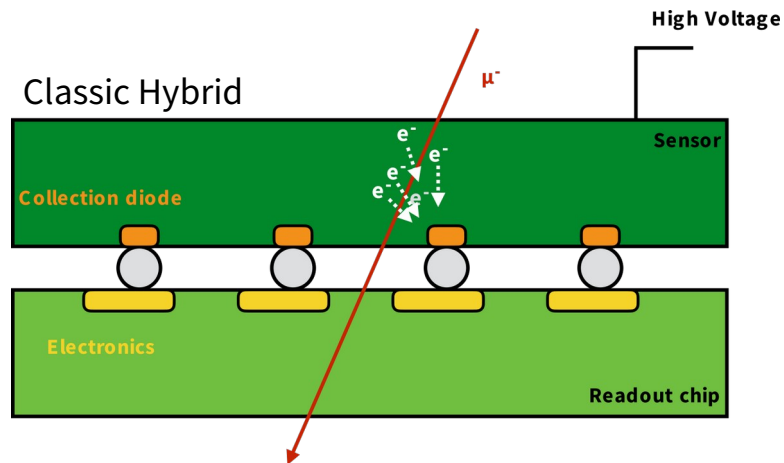


- Segmentation in two dimensions
 - Advantage: Direct 2D spatial measurement, no stereo angles required
 - Disadvantages: Connection to readout electronics, many more channels
- Different technologies, readout concepts, sensor structures
 - Exact design of a sensor very complex (metallization, passivation...)
 - Detectors designed and optimized for specific application (experiment)
- Pixel sizes of a few $10\ \mu\text{m}$ → good spatial resolution
- Sensor thicknesses of a few $100\ \mu\text{m}$ → Little multiple scattering



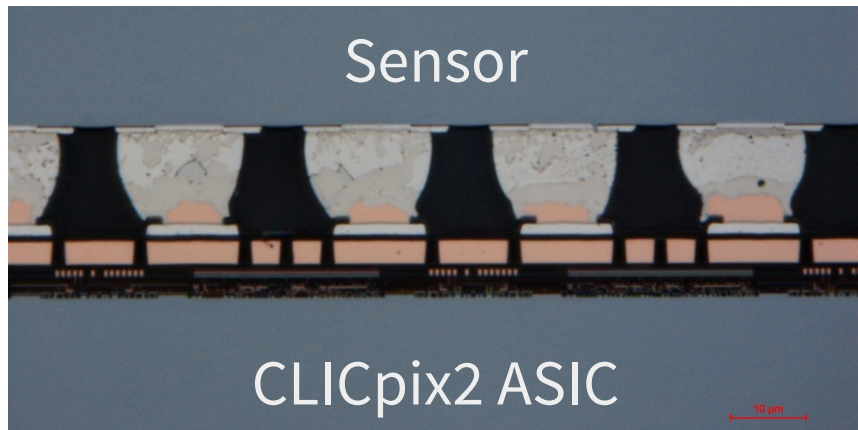
Pixel Detector Technology: Hybrids

- Separation of readout electronics and sensor in two silicon chips
 - Connection via small metal balls (bump bonds) or adhesive layer
 - Sensor doping as desired, high voltage for depletion possible
 - Readout chip can exploit full potential of commercial processes
- Small pixel sizes with lots of functionality possible - but very expensive to produce

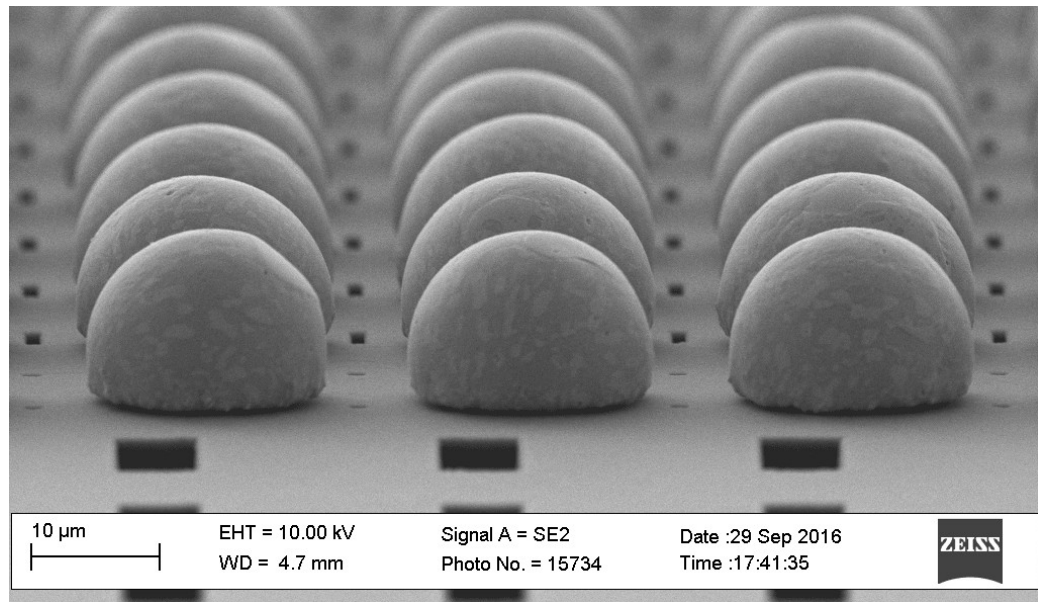


Hybridization: Bump Bond Interconnects

- Different technologies available
- Very common: Bump bonding
 - Size: $\sim 10 - 20 \mu\text{m}$
 - Material: Lead-Tin, Indium, ...



<https://doi.org/10.1088/1748-0221/14/06/C06003>

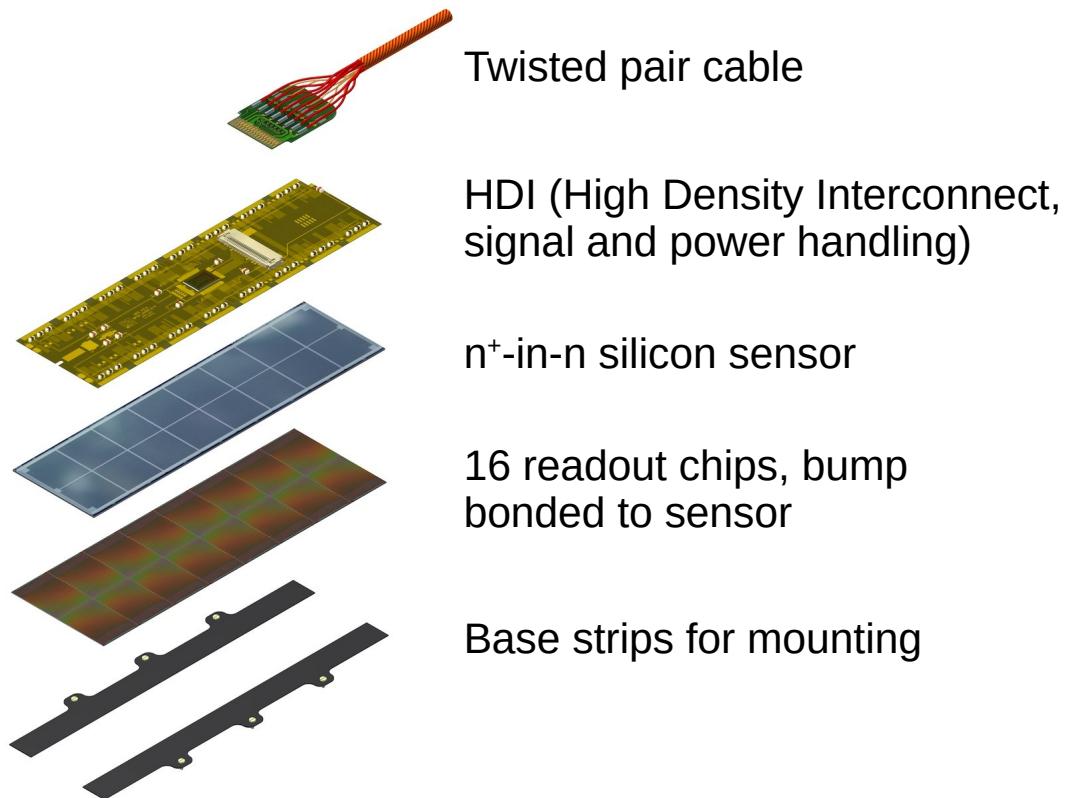


- Different placement techniques
 - Solder spheres \rightarrow individual chips
 - Via lithography \rightarrow wafer-level

A photograph of a Hybrid Silicon Pixel Detector assembly. It features a large, rectangular, off-white sensor chip mounted on a yellow carrier. To the left, a green printed circuit board (PCB) is visible, with numerous gold wire bonds connecting it to the sensor chip. The background is a dark green surface.

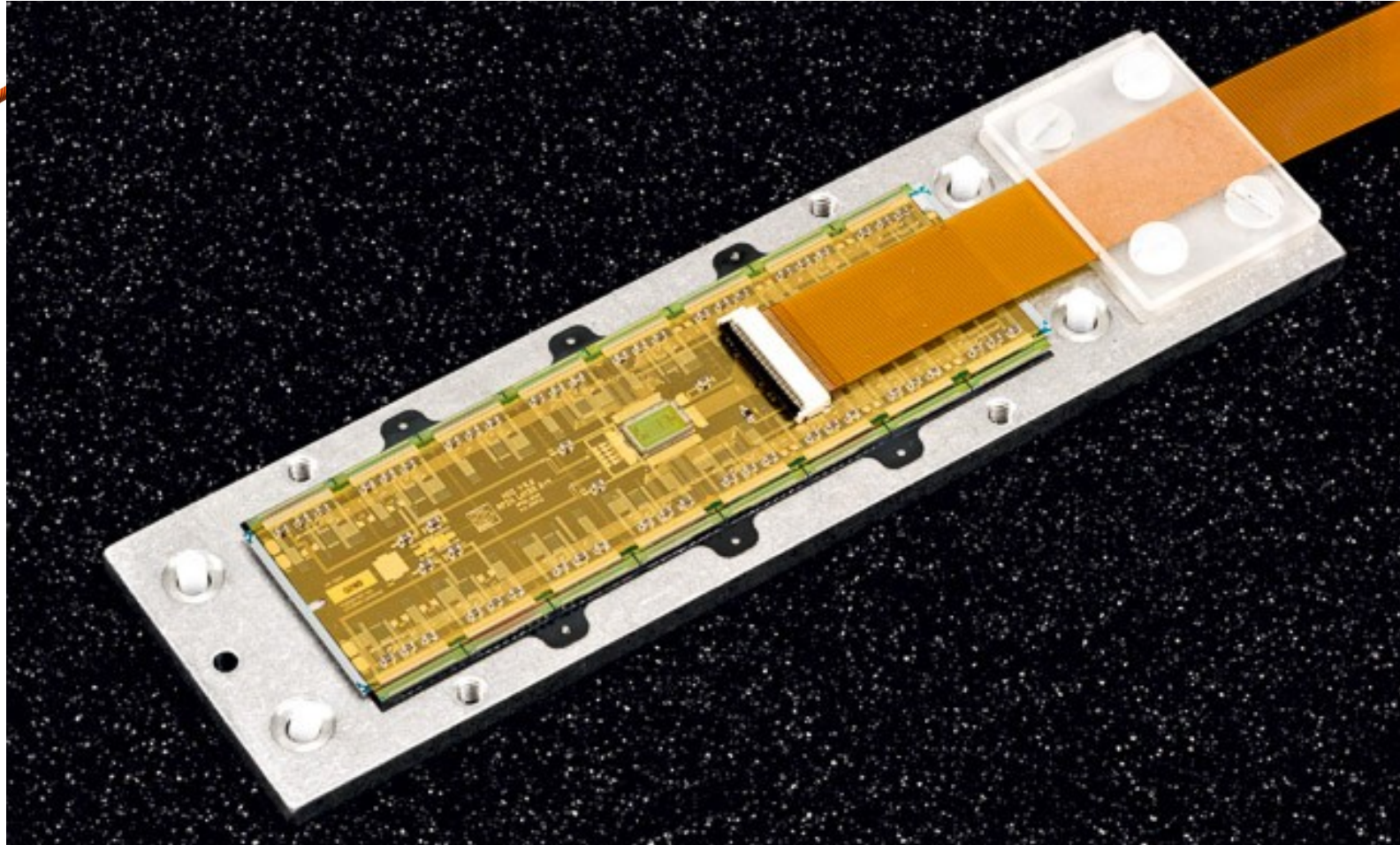
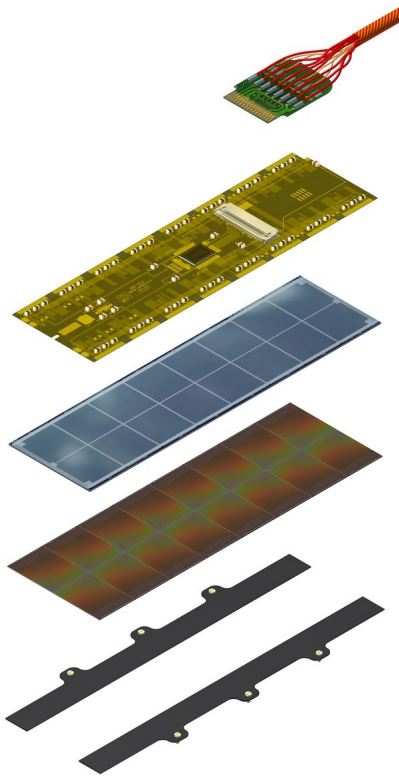
Hybrid Silicon Pixel Detector
100 μm Timepix with 100 μm sensor

Example: CMS Pixel Detector



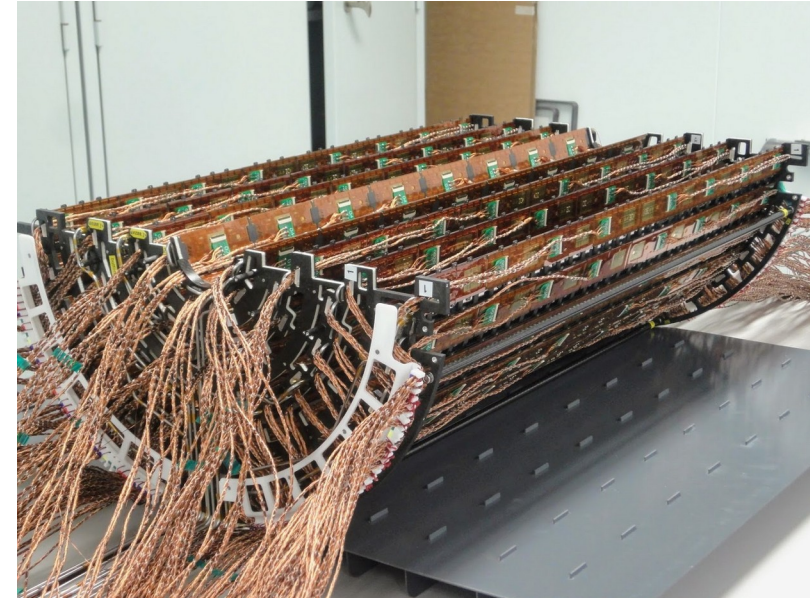
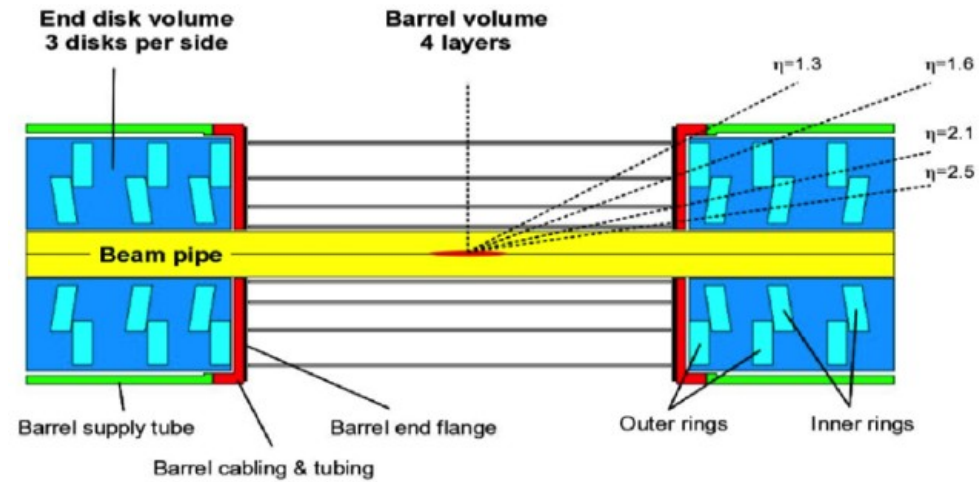
- Sensor:
 - n⁺-in-n sensor technology
 - 285 μm thickness
 - 150 x 100 μm pitch
- Module:
 - 52 x 80 = 4160 pixels/chip
 - 16 chips \rightarrow 4160 x 16 = 66560 pixels/module
 - Total size: 64.8 x 16.2 mm

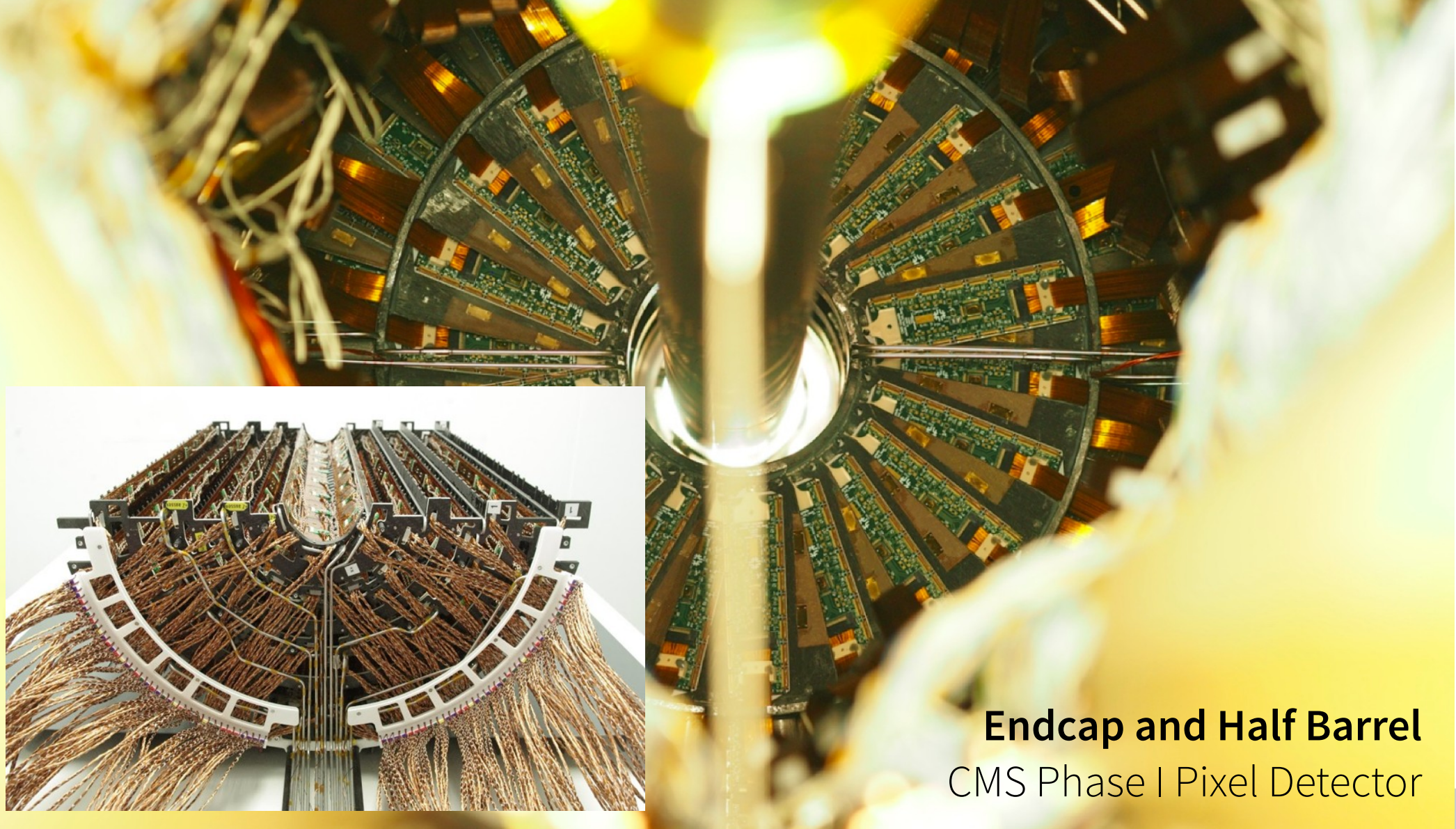
Example: CMS Pixel Detector



Example: CMS Pixel Detector

- Innermost part of the CMS Detector
 - Four *barrel* layers
 - Radii: 3.0, 6.8, 10.2, 16.0 cm
 - Length: 54.9 cm
 - Three *endcap* layers per side
 - Radii: 4.5 – 16.1 cm
- Total number of modules: **1856**
- *124 MPix* – with 25 ns time resolution
- Spatial resolution: $> 5 \mu\text{m}$





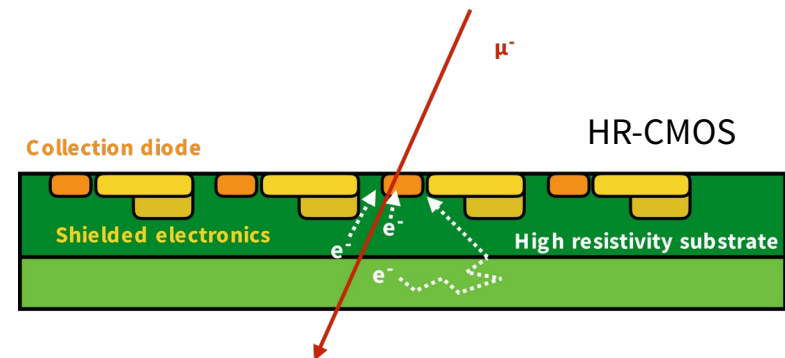
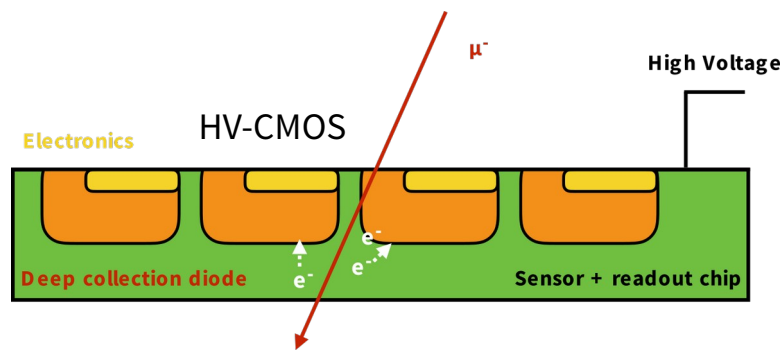
Endcap and Half Barrel
CMS Phase I Pixel Detector



Installation of Phase I Pixel Detector
CMS-Experiment @ LHC

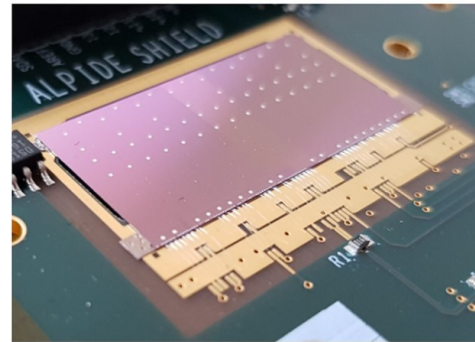
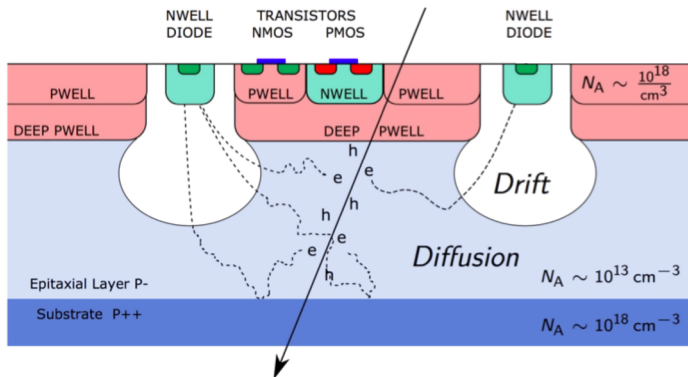
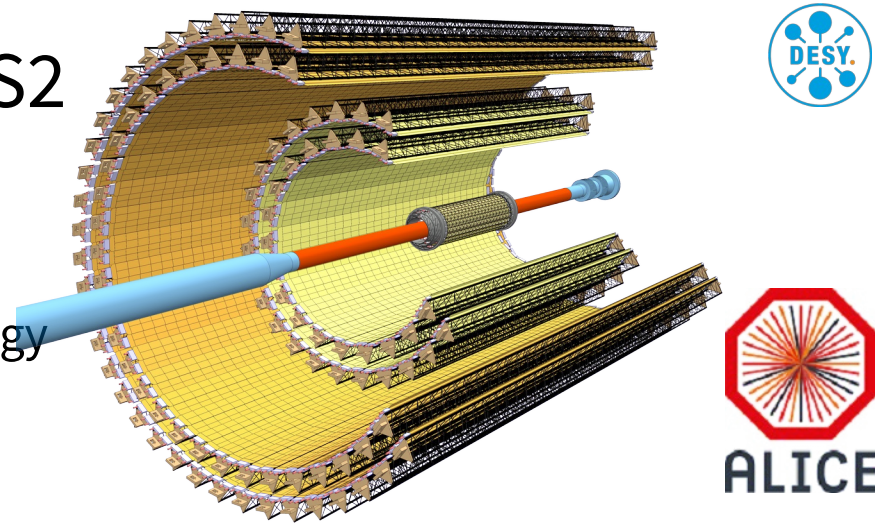
Pixel Detector Technology: Monolithic Sensors

- Goal: minimal material with the greatest possible precision.
- Removal of the readout chip, implementation of the electronics in the sensor
 - Cheaper, because no bump bonding, less material
 - Problem: CMOS electronics can only tolerate low voltage, limited depletion
- Different technologies to isolate "sensor" and "electronics"

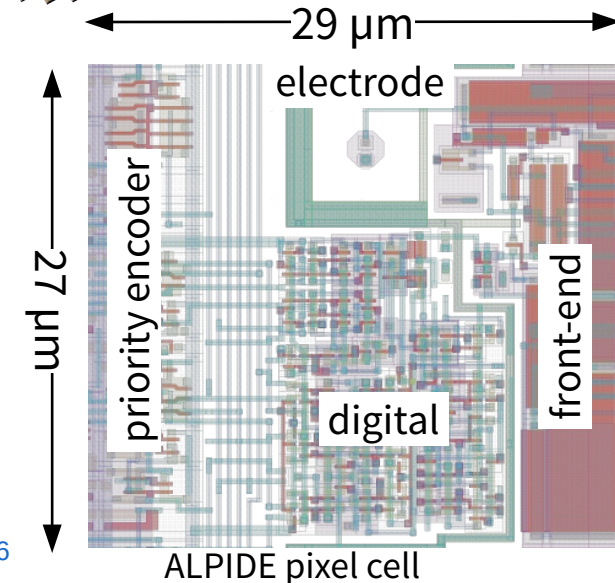


The ALPIDE Sensor of the ALICE ITS2

- Full Inner Tracking System: 24'000 ALPIDE chips, one of the first large-scale detectors with MAPS
- ALPIDE – MAPS in 180 nm CMOS imaging technology
 - 512×1024 pixels, $29 \mu\text{m} \times 27 \mu\text{m}$ pitch
 - Binary detection & readout (hit/no hit)
 - Optimized for low power consumption
 - Produced on epitaxial layers of $18 - 30 \mu\text{m}$

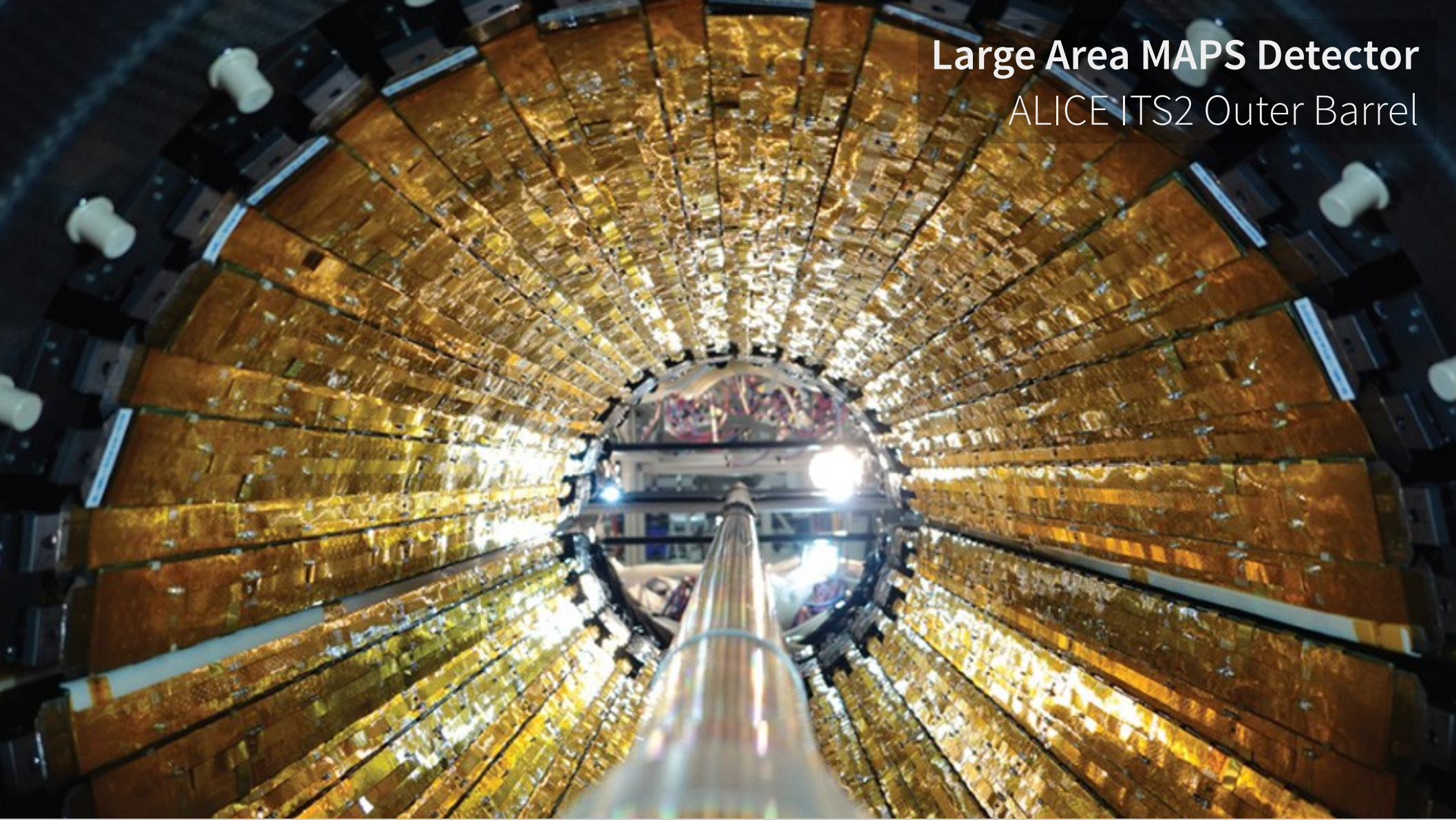


<http://dx.doi.org/10.1016/j.nima.2016.05.016>



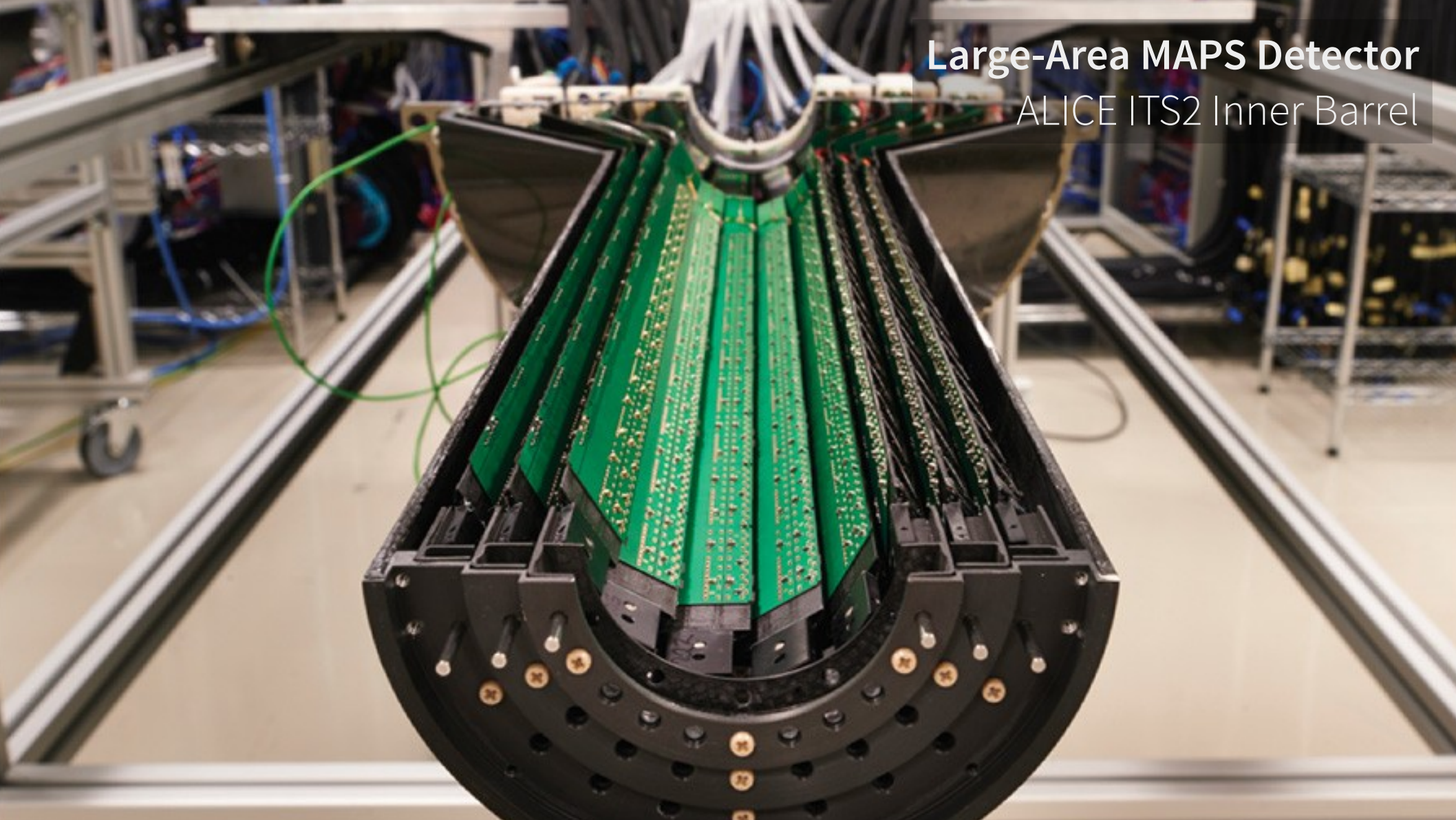
Large Area MAPS Detector

ALICE ITS2 Outer Barrel



Large-Area MAPS Detector

ALICE ITS2 Inner Barrel



Combining Strip & Pixel Detectors

Typical Compromise

- **Pixel detector** at center of experiment
 - Smaller size \rightarrow reduces costs
 - Pixel detector can cope with high occupancy close to IP
- **Strip detector** at larger radii
 - Lower occupancy \rightarrow reduced probability for ghost hits
 - Reduction in number of readout channels

